

Modeling Natural Convection Through RELAP5-3D

A Thesis

Presented in Partial Fulfilment of the Requirements for the

Degree of Master of Science

with a

Major in Mechanical Engineering

in the

College of Graduate Studies

University of Idaho

by

Cody A. Terrill

Major Professor: David Arcilesi, Ph.D.

Committee Members: Richard Christensen, Ph.D.; Michael McKellar, Ph.D.

Department Administrator: Gabriel Potirniche, Ph. D.

December 2022

Abstract

Modeling a system with natural convection being the coolant's primary driving force is frequently challenging due to the programs governing equations not accounting for pressure differences in calculating the mass flow rate. The objective of this project is to create a program that can run a model with the only driving force being the natural convection formed from the pressure difference between an energy sink and an energy source.

To accomplish this the software RELAP5-3D will be used in the one-dimensional format. The model will not have any pumps within the program to ensure the evaluation is capturing only the mass flow rate from the natural convection forces. The only fluid that will be contained within the system is H_2O in both gas and liquid form. The model is divided into four separate executable programs due to the complication of the mass flow rate oscillating during the initial startup of the program.

The results showed that the RELAP program can run a system using pressure differences as the driving force for the mass flow rate of the coolant fluid. The result had uncharacteristic oscillations in both the mass flow rate and temperature of the coolant. This is most likely due to the one-dimensional format of the model. It is recommended to modify to a two-dimensional model to reduce the oscillations within the system.

When comparing to hand calculations there is a considerable difference between the two values. Without the physical model's mass flow rate data to compare, the results are inconclusive as to the accuracy of both evaluation data.

Acknowledgements

I would like to acknowledge Stephen Hancock for his patience and comprehensive support in navigating the RELAP program and manual.

In addition, I would like to give a special thanks to Kevin Terrill for his continued support and encouragement throughout my journey through higher education.

Table of Contents

Abstract	ii
Acknowledgements	iii
Table of Contents	iv
List of Tables	vi
List of Figures	viii
1 Introduction	1
1.1 Background	1
1.2 Motivation and Goal	3
1.3 Approach.....	3
1.4 Scope.....	4
1.5 Problem Statement	4
1.6 Outline	4
2 RELAP5	6
2.1 RELAP History.....	6
2.2 Validity of RELAP	8
2.3 RELAP5-3D One-dimensional Equation.....	15
2.3.1 RELAP5-3D One-Dimensional Disadvantage.....	16
2.3.2 Governing Equations	16
2.3.3 Modifications	25

3	Natural Convection	27
3.1	Modeling Equation.....	28
3.1.1	Navier–Stokes and first law of thermodynamics.....	28
3.1.2	Churchill-Chu Natural Convection Evaluation.....	30
4	Natural Convection Model	32
4.1	Overview	32
4.2	Juncture and branches.....	32
4.2.1	Pressurizer	33
4.2.2	Heat Exchanger Volume	34
4.2.3	Reactor	34
4.2.4	Time Step.....	35
5	Resulting Data	40
5.1	Time Stepped Model.....	40
6	Hand Calculation	45
6.1	Equation	45
6.2	Execution and Resulting Data.....	46
6.3	Physical Model Comparison.....	49
7	Summary and Conclusions	52
	References	54
	Appendix A: Data from the executed programs	60

List of Tables

A.1	500 Watt Time Step	60
A.1	500 Watt Time Step	61
A.1	500 Watt Time Step	62
A.1	500 Watt Time Step	63
A.1	500 Watt Time Step	64
A.1	500 Watt Time Step	65
A.1	500 Watt Time Step	66
A.2	1542 Watt Time Step	66
A.2	1542 Watt Time Step	67
A.2	1542 Watt Time Step	68
A.2	1542 Watt Time Step	69
A.2	1542 Watt Time Step	70
A.2	1542 Watt Time Step	71
A.2	1542 Watt Time Step	72
A.2	1542 Watt Time Step	73
A.3	4452 Watt Time Step	73
A.3	4452 Watt Time Step	74
A.3	4452 Watt Time Step	75
A.3	4452 Watt Time Step	76
A.3	4452 Watt Time Step	77
A.3	4452 Watt Time Step	78
A.3	4452 Watt Time Step	79
A.4	5200 Watt Time Step	80

A.4 5200 Watt Time Step	81
A.4 5200 Watt Time Step	82
A.4 5200 Watt Time Step	83
A.4 5200 Watt Time Step	84
A.4 5200 Watt Time Step	85
A.4 5200 Watt Time Step	86

List of Figures

1.1	Ohmically Heated System (Cut View)	2
2.1	Void Fraction Ratio to Height (5 second)	9
2.2	Void Fraction Ratio to Height (10 second)	10
2.3	Void Fraction Ratio to Height (15 second)	11
2.4	Void Fraction Ratio to Height (20 second)	12
2.5	Void Fraction of the THTF model	13
2.6	Wall Temperature of the THTF model	14
2.7	Vapor Temperature of the THTF model	14
4.1	Graphical returned values of a continuously running program	36
4.2	Mass flow rate of the model with no reactor	37
4.3	Temperature of the model without the heat exchanger	38
4.4	Temperature of the model without the heat exchanger	39
5.1	Mass Flow Rate at all wattage	41
5.2	Mass Flow Rate at 500 Watts	42
5.3	Mass Flow Rate at 1542 Watts	42
5.4	Mass Flow Rate at 4452 Watts	43
5.5	Mass Flow Rate at 5200 Watts	44
6.1	Volume configuration of the hand calculations	47
6.2	Comparative mass flow rates	48
6.3	Physical model at 40 amps	50
6.4	RELAP temperature profile of the 500 watt run	51

CHAPTER 1

Introduction

1.1 Background

This paper uses an ohmically heated system created and designed by the University of Idaho, in partnership with Premier Technology. This model has been created using a pipe inside an annulus. The model is broken down into six main sections: Heater, Chimney, Top branch, Heat exchanger, Return, and Bottom branch. Figure 1.1 shows a cut profile view of the model. The component is filled with heavily salted water. Then there is an electrical current that is run through the heater section of the system. The current that is running through the heater section heats up the water in the area and starts to cause the warmer waters to rise. At first, the convection cycles are only in the heater and chimney location and are isolated through to individual incidences. As the water starts to get hotter the water starts to push into the top branch.

As this starts to happen the natural convection starts to move through the complete system, starting at the heater, then moving through the chimney, reaching the top branch, then moving to the heat exchanger. At the heat exchanger, there are pipes with cool tap water running through the tubes. The heat exchanger is modeled as a standard tube and shell heat exchanger, with the salt water going through the shell, and the cool tap water moving through the tubes. The heat exchanger cools the salt water enough to cause it to drop down the return, and to the Bottom branch. As time passes the saltwater starts to move at a constant mass flow rate through all six sections creating a complete natural circulation loop through the model.

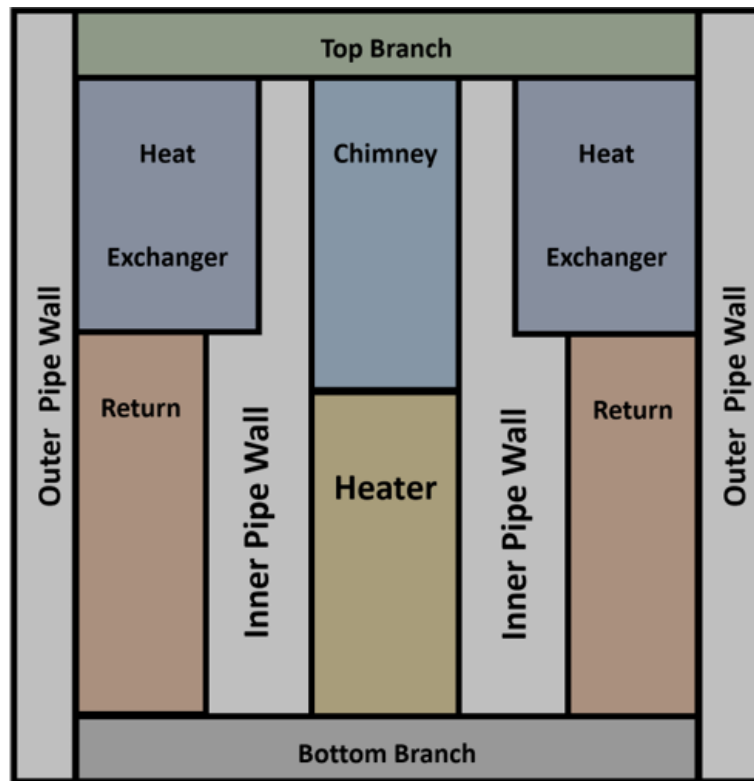


Figure 1.1: Ohmically Heated System (Cut View)

1.2 Motivation and Goal

The motivation for this direction of study comes from the current energy crisis that is faced by the world today. As is commonly discussed and debated the world needs to start moving to cleaner and more renewable energies. As many people can see the use of solar, hydroelectric, and wind energy being clean and renewable there are still many problems with these renewable resources. Ranging from disturbing wildlife's behaviors, environmental impact, and the environmental cost and damage for the initial creation of the equipment, to the inconsistency of power produced throughout the day, and season. With those issues and the ever-increasing need for electrical power in today's modern energy grid, there are many engineering challenges that will need to be achieved in order to meet our world's energy needs.

With these weak points and demands, in many of the green forms of energy, there are many people today, including Microsoft founder Bill Gates, that have spoken out about the value, and need for nuclear energy and its contribution to creating a clean energy grid. The hope of this paper is to create one more piece of research to help assist in creating a safer and more accessible power source for areas of the world where power options are limited.

1.3 Approach

This paper uses the one-dimensional modeling from the RELAP5-3D modeling program. It uses the preset standard elemental properties set within the RELAP5 data. The model was built with standard branches and volumes designed within the RELAP5 program. The coolant fluid was set as H_2O with no additives within the RELAP5 property tables.

1.4 Scope

The topic of this paper focuses on the RELAP5-3D modeling program and all the data contained within the executable program. This paper focuses on the natural circulation of liquid water through the model. This excludes vaporized steam and any other elements. This paper will also exclude any heat or energy transfer from the ambient environment. This will also include excluding any heat or energy transfer through the walls internally in the model.

1.5 Problem Statement

Creating models with natural convection as the driving force is exceptionally challenging. This is common because the governing equations of the modeling programs do not account for the pressure differences to create a mass flow rate. This can cause complications when modeling systems that do not require a pump to create the mass flow of coolant or liquid. This paper will cover a stripped-down and basic ohmic heated system without a pump designed for the cooling system.

1.6 Outline

Chapter 2 covers the RELAP5 program. This includes the history of the RELAP program. The origin of the program, and how it was created. It covers validating data for RELAP5 and the level of accuracy of physical models. Chapter 2 also covers the disadvantage of the one-dimensional modeling of RELAP5. It also covers the governing equations and possible modifiers that can be added to the governing equations.

Chapter 3 focuses on natural convection. This chapter covers the first law of thermodynamics and the core principles that natural convection is based on. Chapter 3 also covers derived equations that have been formed to evaluate the natural circulation.

Chapter 4 covers the RELAP5-3D model that was created to evaluate natural circulation. This includes all the sub-components contained within the model. Chapter 4 also covers the Heating element that was added to the model, and the heat exchanger built. Included in the chapter contains the node's position. Lastly, this chapter covers the general style the program was executed and the justification of why it was executed that way.

Chapter 5 concentrates on the numerical data that was created from the program. This includes evaluation and comparison to the physical behaviors. It also covers similarities and differences between each section of the program.

Chapter 6 contains the same model but is evaluated through hand calculations. It also contains the equations that were used to create the hand-calculated model

CHAPTER 2

RELAP5

2.1 RELAP History

RELAP5 is a program designed by the Idaho National Engineering and Environmental Laboratory (INEEL) for the U.S. Nuclear Regulatory Commission (NRC), in an effort to give the nuclear community a tool that assists in the reactor safety of running nuclear systems. RELAP is an acronym that stands for Reactor Excursion and Leak Analysis Program. The original creation of RELAP started in 1975 under the funding of the Nuclear Regulatory Commission. Later, in 1980, in the aftermath of the Chernobyl nuclear incident RELAP5 was funded by the Department of Energy (DOE) specifically to support the teams that needed to assess the safety of all United States facilities.

RELAP5 would be an electronic model that would allow a more complete evaluation and assessment without needing to run the risk of running tests in the physical facility. Post-Chernobyl the Department of Energy performed a re-assessment of the safety of all its reactors throughout the United States. RELAP5 played an essential role in evaluating the thermal hydraulic analysis of the primary coolant system, of both boiling water reactors (BWR), pressure water reactors (PWR), and many other experimental designs. From that point, RELAP5 has become known as the world standard for thermal-hydraulic evaluations in the nuclear community.

Through the evaluation of these systems throughout the United States Department of Energy, there were many aspects that RELAP5 could be improved on. Some of these aspects were the need for new modeling capabilities, a three-dimensional flow model, heavy water properties added to the capability, a new critical heat flux cor-

relation, unique fuel designs, and many other smaller features. This need drove the Department of Energy to support a multi-million dollar investment in the RELAP program. In 1995 RELAP5 started to have an issue with varying and contradicting needs presented to it. In response to the growing needs, the RELAP program was split into two separate versions. The INEEL focused on the future versions being backward compatible with legacy models, to ensure the RELAP program can still be reliable for validation, with the models created in the 1980s.

The first version would be controlled by the Nuclear Regulatory Commission (NRC). It would be called RELAP5 MOD 3.2. With the second version being controlled by the Department of Energy (DOE). That version would be called RELAP5-3D. This model and all analyses of this model were created using the Department of Energy Version, RELAP-3D. The main changes between the two versions mainly consisted of the RELAP5 in the multi-dimensional versions. This model will only utilize the one-dimensional modeling so it should be compatible with RELAP5 MOD 3.2 if necessary. Due to similarities, the entirety of the deviations can be ignored as long as the evaluation stays in the one-dimensional modeling of the RELAP5 program.

From the beginning, there have been eighteen different updated versions of RELAP. For this model, the most up-to-date version will be used, version 4.4.2ie. This version was distributed through Battelle Energy Alliance LLC, through the Idaho National Laboratory (INL). Under Contract DE-AC07-05ID14517 with the United States Department of Energy, the current authorized distributor of the RELAP5-3D code.

2.2 Validity of RELAP

There have been several validation tests have been performed on the accuracy of the RELAP models. With that in mind, there are two tests that focus heavily on one-dimensional modeling compared to multi-dimensional modeling. Due to this model being a one-dimensional model these two tests will be focused on the validity of the RELAP5-3D program.

The first test is from G.E. Level Swell. This test analyzed the flashing and inter-phase drag of a fluid. To perform this test G.E. Level Swell took two fully enclosed tanks, and connected them to a blowdown valve, with differential pressure sensors, vertically aligned along the tanks. Then the two tanks were filled partially with water. The tanks were sealed and then the heat was added to the water in the tanks until they reached the edge of the saturation point. The blowdown valves were then opened causing the pressure in the tank to drop and pushing the water in the tank past the saturation point. As the tanks were depressurized through the blowdown valve the differential pressure sensors analyzed the average void fraction as a function of the elevation in the tank.

This data was then compared to a RELAP5 MOD3.2 and RELAP5 3D model. The data was then graphed four times during the blowdown, 5 seconds Figure 2.1, 10 seconds Figure 2.2, 15 seconds Figure 2.3, and 20 seconds Figure 2.4. The figures show the results of the 4-foot tank experiment. This shows that the two forms of RELAP5 are identical. This also shows that the RELAP5 models correctly mimic and display true values within the standard deviation of the equipment's accuracy.

The second test was performed by the Thermal Hydraulic Test Facility (THTF), by conducting an experiment that simulated a pressurized water reactor (PWR). This

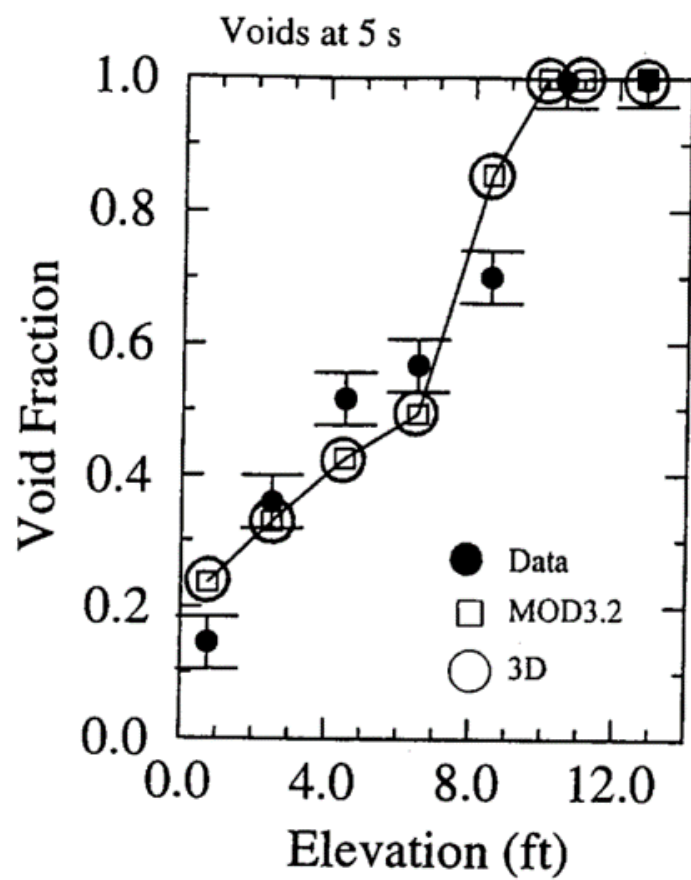


Figure 2.1: Void Fraction Ratio to Height (5 second)

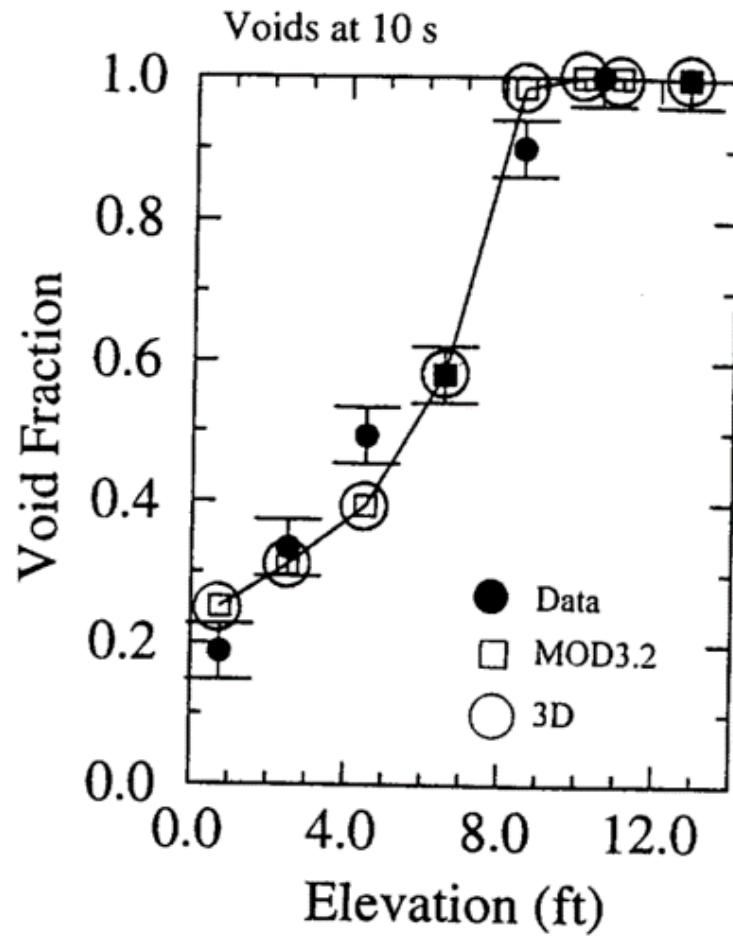


Figure 2.2: Void Fraction Ratio to Height (10 second)

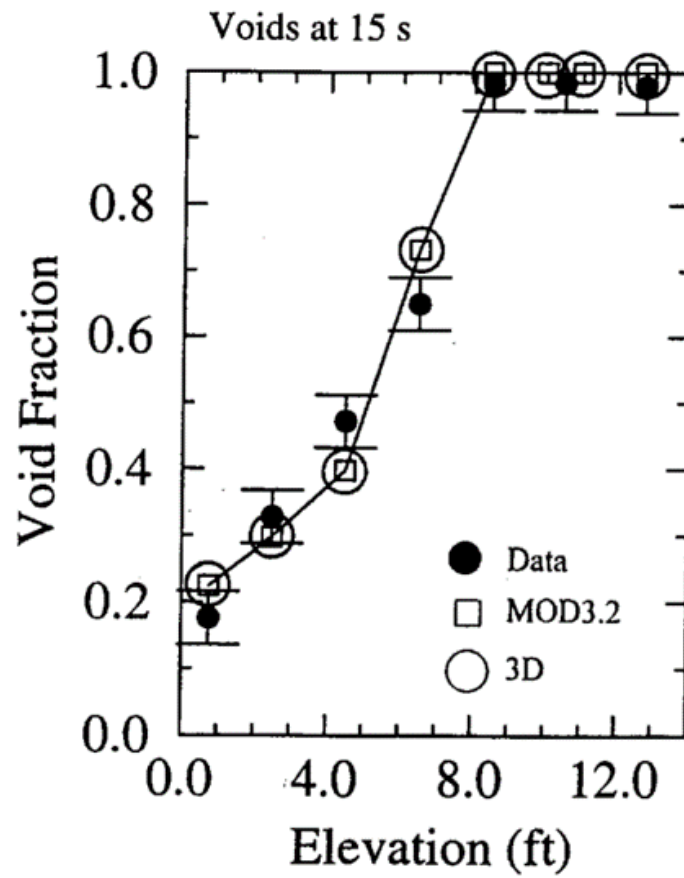


Figure 2.3: Void Fraction Ratio to Height (15 second)

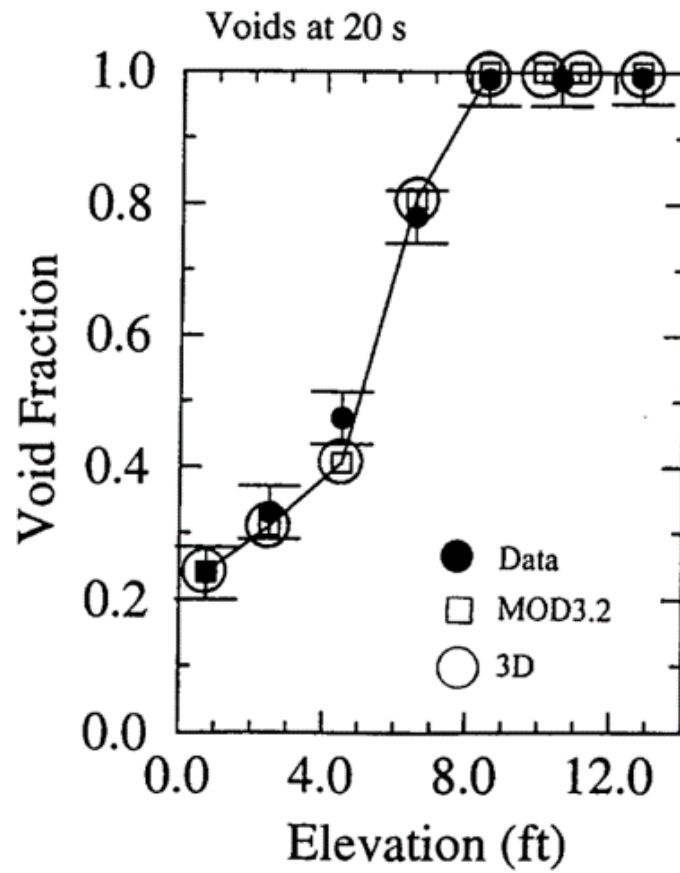


Figure 2.4: Void Fraction Ratio to Height (20 second)

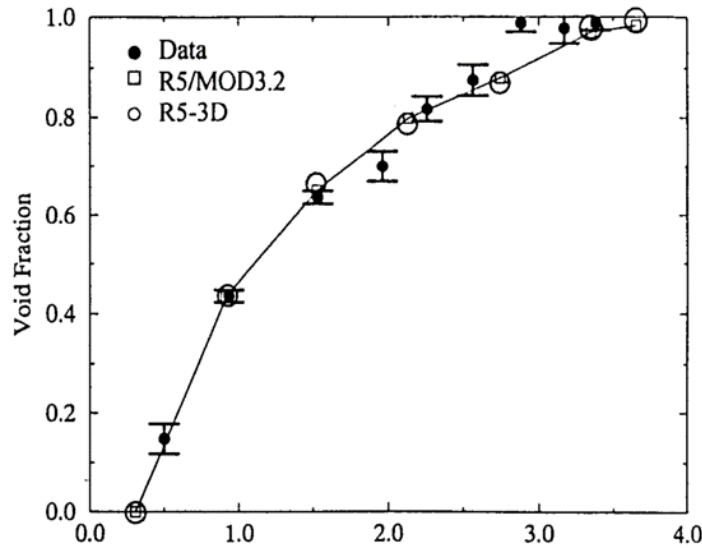


Figure 2.5: Void Fraction of the THTF model

test contained 64 electrically heated rods, simulating fuel rods in a PWR. The rods were aligned in a 17 by 17 square arrangement. The test had differential pressure sensors and thermocouples aligned through the inside of the chamber. These sensors were used to measure the void fractions, the thermal temperature of the wall, and the thermal temperature of the steam. The test was performed at 4.5 MPa, with an inlet mass flux of $29.8 \frac{Kg}{m^2 \cdot Sec}$, and inlet sub-cooling at 57.6 K. after this test was run, a model was created with both RELAP5 MOD3.2, and RELAP5 3D.

When the model was created it was then compared and graphed for the three criteria. First the Void fraction Figure 2.5. Then the Wall Temperature Figure 2.6. Finally, the Vapor Temperature Figure 2.7. As the data has shown the two versions of RELAP are almost identical in the first few meters, and extraordinarily close for the last few meters. This analysis also showed RELAP accurate to the physical model within reasonable deviation.

The accuracy between the two RELAP5 models can be mainly contributed to the

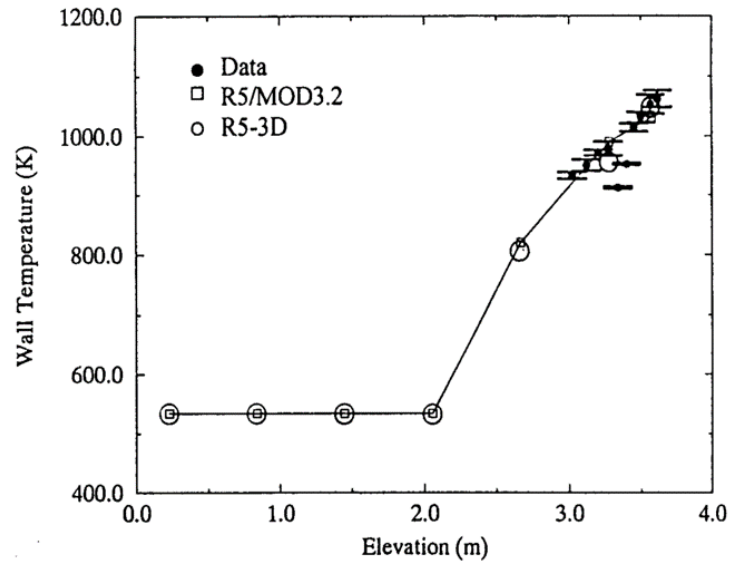


Figure 2.6: Wall Temperature of the THTF model

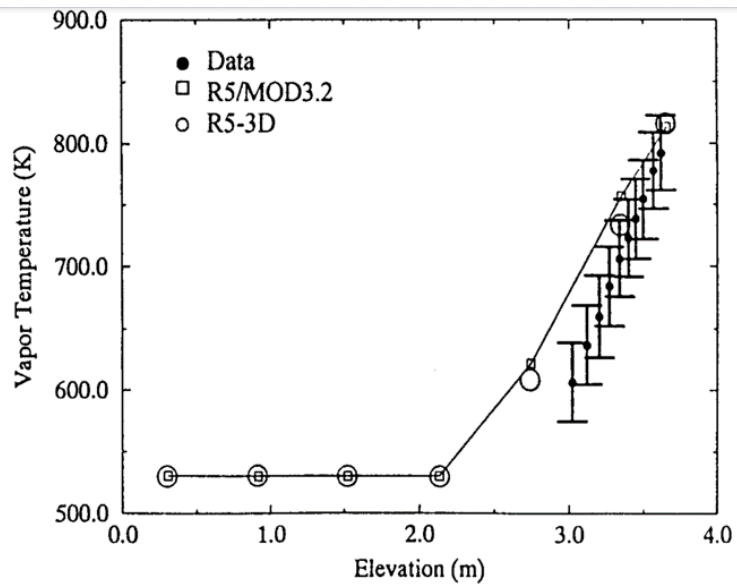


Figure 2.7: Vapor Temperature of the THTF model

choice of how the models are created. In both models, the RELAP5 one-dimensional modeling was applied. If the models were created in the multi-dimensional modeling format the similarities could vary considerably. That is due to the one-dimensional modeling having a very small number of deviations between the two programs, RELAP5 3D and RELAP5 MOD3.2.

2.3 RELAP5-3D One-dimensional Equation

RELAP5-3D in one dimension is governed by a series of finite elements. Due to the complicated nature of both thermodynamics and fluid mechanics, the RELAP5-3D in one dimension is processed through a series of nodes connected by interlocking mesh components. The primary advantage of this method is the speed and computing power required are considerably reduced. As a model is created, the larger and more complicated it becomes the required computing power necessary to analyze the model will exponentially grow. This issue requires a longer computing time, or in some cases a supercomputer to process the model and data accurately.

This will increase the cost of the analysis The cost will increase considerably if a supercomputer is required; due to supercomputers requiring a substantial amount of maintenance and having a high depreciation rate. Because of this, and the ease of obtaining a legal and valid software license from the Department of Energy, RELAP5-3D has become one of the most valid and widely used software throughout the Nuclear community.

2.3.1 RELAP5-3D One-Dimensional Disadvantage

Like many programs, there are some disadvantages to RELAP5-3D. The primary disadvantage of RELAP5 is the awkward and difficult user interface. The primary coding program is built and created around the concept of 'cards'. Within each card, there are specific commands called 'words' that will decipher how the code is constructed or altered. This unique format makes RELAP5 one of the more difficult programs to operate and work with. Most other Analysis software is very visual, with multiple different ways to interact with the components and properties; for example, Solidworks, and Aspen HYSYS. The Idaho National Laboratory (INL) attempts to mitigate this issue by using a very inclusive and comprehensible set of manuals to help users walk through the program.

The second disadvantage of RELAP5 is using a node and mesh analysis. Simplifying a 3-dimensional model, with a finite time window, to a simple node-to-node connection considerably reduces the complexity of the actions happening within the model. This in turn creates a risk of a loss of accuracy due to oversimplification. RELAP5-3D combats this by using a complex set of governing equations and optional modifiers to adjust the equation according to special situations. If done correctly this should reduce the margin of error within the range of acceptable values.

2.3.2 Governing Equations

The thirteen primary equations are broken down into these nine separated but connected categories, the sum continuity equation, the difference continuity equation, the total noncondensable continuity equation, the vapor/gas thermal energy equation, the liquid thermal energy equation, the donor quantities equation, linearizing the phasic

density, the provisional advanced time heat transferred rate equation, and the provisional advanced time heat temperature rate equation. RELAP5 uses the thirteen equations to be able to cleanly transition the thermodynamic and fluid mechanic properties from one mesh node to another.

The sum continuity equation

Equation 2.1 is the base for the Momentum equation. The sum continuity equation is evaluated with the difference continuity equation with the superscript of n setting the time level index.

$$\begin{aligned}
 & V_L[\alpha_{g,L}^n(\tilde{\rho}_{g,L}^{n+1} - \rho_{g,L}^n) + \alpha_{f,L}^n(\tilde{\rho}_{f,L}^{n+1} - \rho_{f,L}^n) + (\rho_{g,L}^n - \rho_{f,L}^n)(\tilde{\alpha}_{g,L}^{n+1} - \alpha_{g,L}^n)] \\
 & \quad + (\dot{\alpha}_{g,j+1}^n \dot{\rho}_{g,j+1}^n v_{g,j+1}^{n+1} A_{j+1} - \dot{\alpha}_{g,j}^n \dot{\rho}_{g,j}^n * V_{g,j}^{n+1} A_j) * \Delta t \quad (2.1) \\
 & \quad - (\dot{\alpha}_{f,j+1}^n \dot{\rho}_{f,j+1}^n v_{f,j+1}^{n+1} A_{j+1} - \dot{\alpha}_{f,j}^n \dot{\rho}_{f,j}^n * V_{f,j}^{n+1} A_j) * \Delta t = 0
 \end{aligned}$$

V_L is the volume of the measured length; $\alpha_{g,L}^n$ is the volume fraction of the gas within the measured length; $\tilde{\rho}_{g,L}^{n+1}$ is the density of the gas of the measured length in the intermittent time step; $\rho_{g,L}^n$ is the density of the gas of the measured length within the measured length bound to the current time step; $\alpha_{f,L}^n$ is the volume fraction of the fluid within the measured length; $\tilde{\rho}_{f,L}^{n+1}$ is the density of the fluid of the measured length in the intermittent time step; $\rho_{f,L}^n$ is the density of the fluid of the measured length within the measured length bound to the current time step; $\tilde{\alpha}_{g,L}^n$ is the volume fraction of the gas within the measured length in the intermittent time step; $\dot{\alpha}_{g,j+1}^n$ is the volume fraction of the gas from the donor quantity of the next noted junction j; $\dot{\rho}_{g,j+1}^n$ is the density of the gas from the donor quantity of the next noted junction j;

$v_{g,j+1}^{n+1}$ is the velocity of the gas of the next noted junction; A_{j+1} is the cross-sectional area of the next noted junction; $\alpha_{g,j}^n$ is the volume fraction of the gas from the donor quantity of the noted junction j ; $\dot{\rho}_{g,j}^n$ is the density of the gas from the donor quantity of the noted junction j ; $v_{g,j+1}^n$ is the velocity of the gas of the noted junction; A_j is the cross-sectional area of the next junction; Δt is the increment in time variable; $\alpha_{f,j}^n$ is the volume fraction of the fluid from the donor quantity of the noted junction j ; $\dot{\rho}_{f,j}^n$ is the density of the fluid from the donor quantity of the noted junction j ; $v_{f,j}^n$ is the velocity of the fluid of the noted junction; $\alpha_{f,j+1}^n$ is the volume fraction of the fluid from the donor quantity of the next noted junction j ; $\dot{\rho}_{f,j+1}^n$ is the density of the fluid from the donor quantity of the next noted junction j ; $v_{f,j+1}^n$ is the velocity of the fluid of the next noted junction;

The difference continuity equation

The difference continuity equation (Equation 2.2) is the complimentary equation to Equation 2.1 with the superscript of n setting the time level index.

$$\begin{aligned}
& V_L[\alpha_{g,L}^n(\tilde{\rho}_{g,L}^{n+1} - \rho_{g,L}^n) + \alpha_{f,L}^n(\tilde{\rho}_{f,L}^{n+1} - \rho_{f,L}^n) + (\rho_{g,L}^n - \rho_{f,L}^n)(\tilde{\alpha}_{g,L}^{n+1} - \alpha_{g,L}^n)] \\
& \quad + (\dot{\alpha}_{g,j+1}^n \dot{\rho}_{g,j+1}^n v_{g,j+1}^{n+1} A_{j+1} - \dot{\alpha}_{g,j}^n \dot{\rho}_{g,j}^n * V_{g,j}^{n+1} A_j) * \Delta t \\
& \quad - (\dot{\alpha}_{f,j+1}^n \dot{\rho}_{f,j+1}^n v_{f,j+1}^{n+1} A_{j+1} - \dot{\alpha}_{f,j}^n \dot{\rho}_{f,j}^n * V_{f,j}^{n+1} A_j) * \Delta t = \\
& - \left(\frac{2}{h_g^* - h_f^*} \right) V_L \Delta t \left[\frac{P_{s,L}^n}{P_L^n} H_{ig,L}^n (\tilde{T}_L^{s,n+1} - \tilde{T}_{g,L}^{s,n+1}) + H_{if,L}^n (\tilde{T}_L^{s,n+1} - \tilde{T}_{f,L}^{s,n+1}) \right] + 2V_L \Delta t \Gamma_{w,L}^n
\end{aligned} \tag{2.2}$$

The undefined variables are as follows ($VALUE_L^n$) the value is within the measured length; h_g^* is the special enthalpy of the gas; h_f^* is the special enthalpy of the liquid;

$P_{s,L}^n$ is the pressure of the vapor/gas phase within the measured length; P_L^n is the pressure of the liquid within the measured length; $H_{ig,L}^n$ is the interface fluid head of the gas within the measured length; $\tilde{T}_L^{s,n+1}$ is the temperature of the saturation property within the measured length in the intermittent time step; $\tilde{T}_{g,L}^{s,n+1}$ is the temperature of the gas within the measured length in the intermittent time step; $H_{if,L}^n$ is the interface fluid head of the liquid within the measured length; $\tilde{T}_{f,L}^{s,n+1}$ is the temperature of the fluid within the measured length in the intermittent time step; $\Gamma_{w,L}^n$ volumetric mass exchange rate within the measured length;

The total noncondensable continuity equation

The total noncondensable continuity equation (Equation 2.3) is used to evaluate the none condensate elements within the system. elements that are either too far above or below the saturation point to be able to change states.

$$\begin{aligned} V_L[\rho_{g,L}^n X_{g,L}^n (\tilde{\alpha}_{g,L}^{n+1} - \alpha_{g,L}^n) + \alpha_{g,L}^n X_{g,L}^n (\tilde{\rho}_{g,L}^{n+1} - \rho_{g,L}^n) + \alpha_{g,L}^n \rho_{g,L}^n (\tilde{X}_{g,L}^{n+1} - X_{g,L}^n)] \\ + (\dot{\alpha}_{g,j+1}^n \dot{\rho}_{g,j+1}^n \dot{X}_{n,j+1}^n v_{g,j+1}^{n+1} A_{j+1} - \dot{\alpha}_{g,j}^n \dot{\rho}_{g,j}^n \dot{X}_{n,j}^n v_{g,j}^{n+1} A_j) \Delta t = 0 \end{aligned} \quad (2.3)$$

The undefined variables are as follows $X_{g,L}^n$ is the mass fraction of the noncondensable gas in the measured length; $\tilde{X}_{g,L}^{n+1}$ is the mass fraction of the gas from the donor quantity of the next noted junction j; $\dot{X}_{n,j+1}^n$ is the mass fraction of noncondensable gas from the donor quantity at the current time junction j within the measured length; $\dot{X}_{n,j}^n$ is the mass fraction of noncondensable gas from the donor quantity at the next time junction j within the measured length; $v_{g,j}^{n+1}$ is the kinematic viscosity of the gas in the current time junction j within the measured length;

The vapor/gas thermal energy equation

The vapor/gas thermal energy equation (Equation 2.4) is the equation that balances the energy stored, and transported through the gas, and vapors in the model.

$$\begin{aligned}
& V_L[(\rho_{g,L}^n U_{g,L}^n + P_L^n)(\tilde{\alpha}_{g,L}^{n+1} - \alpha_{g,L}^n) + \alpha_{g,L}^n U_{g,L}^n (\tilde{\rho}_{g,L}^{n+1} - \rho_{g,L}^n) + \alpha_{g,L}^n \rho_{g,L}^n (\tilde{U}_{g,L}^{n+1} - U_{g,L}^n)] \\
& \quad + [\dot{\alpha}_{g,j+1}^n (\dot{\rho}_{g,j+1}^n \dot{U}_{g,j+1}^n + P_L^n) v_{g,j+1}^{n+1} A_{j+1} - \dot{\alpha}_{g,j}^n (\dot{\rho}_{g,j}^n \dot{U}_{g,j}^n + P_L^n) v_{g,j}^{n+1} A_j] \Delta t \\
& = [- (\frac{h_f^*}{h_g^* - h_f^*})_L^n \frac{P_{s,L}^n}{P_L^n} H_{ig,L}^n (\tilde{T}_L^{s,n+1} - \tilde{T}_{g,L}^{n+1}) - (\frac{h_f^*}{h_g^* - h_f^*})_L^n H_{if,L}^n (\tilde{T}_L^{s,n+1} - T_{f,L}^{n+1}) \\
& \quad \frac{P_L^n - P_{s,L}^n}{P_L^n} H_{gf,L}^n (\tilde{T}_{g,L}^{n+1} - \tilde{T}_{f,L}^{n+1}) + [\frac{1+\varepsilon}{2} h'_{g,L}{}^n + \frac{1-\varepsilon}{2} h'_{f,L}{}^n] \Gamma_{w,L}^n + Q_{wg,L}^n + DISS_{g,L}^n] V_L \Delta t
\end{aligned} \tag{2.4}$$

The undefined variables are as follows $U_{g,L}^n$ is the specific internal energy of the gas at the current time step within the measured volume; P_L^n is the Pressure at the current time step within the measured volume; $\tilde{U}_{g,L}^{n+1}$ is the specific internal energy of gas within the measured volume at an intermediate time variable; $\dot{U}_{g,j+1}^n$ is the specific internal energy of the gas from the donor quantity from the forward junction at the current time junction; $\dot{U}_{g,j}^n$ is the specific internal energy of the gas from the donor quantity from the starting junction at the current time junction; $H_{gf,L}^n$ is the volumetric heat transfer coefficient of the phasic difference within the measured volume at the current time junction; $\tilde{T}_{g,L}^{n+1}$ is the temperature of the gas within the measured volume at an intermediate time variable; $\tilde{T}_{f,L}^{n+1}$ is the temperature of the liquid within the measured volume at an intermediate time variable; $h'_{g,L}{}^n$ is the specific enthalpy of the gas based on the total mixture mass within the measured volume at the current time junction; $h'_{f,L}{}^n$ is the specific enthalpy of the liquid based on the total

mixture mass within the measured volume at the current time junction; $Q_{wg,L}^n$ is the volumetric heat addition rate of the wall to gas within the measured volume at the current time junction; ε is the coefficient of the heat transfer rate of the wall of the pipe, and the fluid; $DISS_{g,L}^n$ is the energy dissipation function of the gas within the measured volume at the current time junction;

The liquid thermal energy equation

The liquid thermal energy equation (Equation 2.5) is the complementary equation to equation 2.4. This equation evaluates the energy stored and transported in the liquids within the model.

$$\begin{aligned}
& V_L [-(\rho_{g,L}^n U_{g,L}^n + P_L^n)(\tilde{\alpha}_{g,L}^{n+1} - \alpha_{g,L}^n) + \alpha_{g,L}^n U_{g,L}^n (\tilde{\rho}_{g,L}^{n+1} - \rho_{g,L}^n) + \alpha_{g,L}^n \rho_{g,L}^n (\tilde{U}_{g,L}^{n+1} - U_{g,L}^n)] \\
& \quad + [\dot{\alpha}_{g,j+1}^n (\dot{\rho}_{g,j+1}^n \dot{U}_{g,j+1}^n + P_L^n) v_{g,j+1}^{n+1} A_{j+1} - \dot{\alpha}_{g,j}^n (\dot{\rho}_{g,j}^n \dot{U}_{g,j}^n + P_L^n) v_{g,j}^{n+1} A_j] \Delta t \\
& = [(\frac{h_f^*}{h_g^* - h_f^*})_L^n \frac{P_{s,L}^n}{P_L^n} H_{ig,L}^n (\tilde{T}_L^{s,n+1} - \tilde{T}_{g,L}^{n+1}) + (\frac{h_f^*}{h_g^* - h_f^*})_L^n H_{if,L}^n (\tilde{T}_L^{s,n+1} - T_{f,L}^{n+1}) \\
& \quad + \frac{P_L^n - P_{s,L}^n}{P_L^n} H_{gf,L}^n (\tilde{T}_{g,L}^{n+1} - \tilde{T}_{f,L}^{n+1}) - \\
& \quad \quad \quad [\frac{1 + \varepsilon}{2} h'_{g,L}{}^n + \frac{1 - \varepsilon}{2} h'_{f,L}{}^n] \Gamma_{w,L}^n + Q_{wg,L}^n + DISS_{g,L}^n] V_L \Delta t
\end{aligned} \tag{2.5}$$

The donored quantities equation

The donored quantities equation (Equation 2.6) is based on the velocity of the junctions created. The donor quantities equation is a volume average scalar value. This creates a simple average between components within the model.

$$\dot{\Phi}_j = \frac{1}{2}(\Phi_K + \Phi_L) + \frac{1}{2} \frac{|V_j|}{V_j} (\Phi_K - \Phi_L) \quad (2.6)$$

The undefined variables are as follows $\dot{\Phi}_j$ is Roe's superbee gradient limiter from the donor quantity from the starting junction; Φ_K is Roe's superbee gradient limiter for the spatially nodded volume index; Φ_L is Roe's superbee gradient limiter for the spatially nodded laminar volume index; V_j is the specific volume from the starting junction; $|V_j|$ is the absolute value of the specific volume from the starting junction;

Linearizing the phasic density

To accomplish a provisionally advanced time phasic density equation 2.7, and equation 2.8 are used, linearizing the phasic density. These two equations create a two-term two-term Taylor series expansion. These two equations are then evaluated to find the fluid density of the gas/vapor, liquid, and noncondensable gas.

$$\tilde{\rho}_{g,L}^{n+1} = \rho_{g,L}^n + \left(\frac{\partial \rho_g}{\partial P}\right)_L^n (P_L^{n+1} - P_L^n) + \left(\frac{\partial \rho_g}{\partial X_n}\right)_L^n (\tilde{X}_{n,L}^{n+1} - X_{n,L}^n) + \left(\frac{\partial \rho_g}{\partial U_g}\right)_L^n (\tilde{U}_{g,L}^{n+1} - U_{g,L}^n) \quad (2.7)$$

$$\tilde{\rho}_{f,L}^{n+1} = \rho_{f,L}^n + \left(\frac{\partial \rho_f}{\partial P}\right)_L^n (P_L^{n+1} - P_L^n) + \left(\frac{\partial \rho_f}{\partial U_f}\right)_L^n (\tilde{U}_{f,L}^{n+1} - U_{f,L}^n) \quad (2.8)$$

The undefined variables are as follows $\left(\frac{\partial \rho_g}{\partial P}\right)_L^n$ is the partial derivative of the density of the gas with respect to the pressure within the measured volume at the current time junction; P_L^{n+1} is the pressure within the measured volume of the next noted junction j; $\left(\frac{\partial \rho_g}{\partial X_n}\right)_L^n$ is the partial derivative of the density of the gas with respect to the flow quality of the noncondensable component of vapor within the measured volume at the current time junction; $\tilde{X}_{n,L}^{n+1}$ is the mass fraction of the noncondensable gas

in the measured volume at an intermittent time step at the next time level index; $X_{n,L}^n$ is the mass fraction of the noncondensable gas in the measured volume at the current time level index; $(\frac{\partial \rho_g}{\partial U_g})_L^n$ is the partial derivative of the density of the gas with respect to the specific internal energy of the gas within the measured volume at the current time junction; $\tilde{U}_{g,L}^{n+1}$ is the specific internal energy of the gas in the measured volume at an intermittent time step at the next time level index; $U_{g,L}^n$ is the specific internal energy in the gas in the measured volume at the current time level index; $\tilde{\rho}_{f,L}^{n+1}$ is the density of the liquid in the measured volume at an intermittent time step at the next time level index; $(\frac{\partial \rho_f}{\partial P})_L^n$ is the partial derivative of the density of the fluid with respect to the pressure within the measured volume at the current time junction; P_L^{n+1} is the pressure in the measured volume at the next time level index; $(\frac{\partial \rho_f}{\partial U_f})_L^n$ is the partial derivative of the density of the liquid with respect to the specific internal energy of the liquid within the measured volume at the current time junction; $\tilde{U}_{f,L}^{n+1}$ is the specific internal energy of the fluid in the measured volume at an intermittent time step at the next time level index; $U_{f,L}^n$ is the specific internal energy in the liquid in the measured volume at the current time level index;

The provisional advanced time phasic interface heat transfer rates

The provisional advanced time phasic interface heat transfer rates are given through equation 2.9 and equation 2.10. These two equations find the rate of heat transfer for the gas/vapor of the fluid, the liquid fluid, the noncondensable gas, and the outer wall holding the fluid. This is extrapolated using the finite difference form of the first law of thermodynamics and the total vapor/gas interface energy transfer

$$\tilde{Q}_{ig,L}^{n+1} = \frac{P_{s,L}^n}{P_L^n} H_{ig,L}^n (\tilde{T}_L^{s,n+1} - \tilde{T}_{g,L}^{n+1}) - \left(\frac{1-\varepsilon}{2}\right) \Gamma_{w,L}^n (\dot{h}_{g,L}^n - \dot{h}_{f,L}^n) \quad (2.9)$$

$$\tilde{Q}_{ig,L}^{n+1} = H_{ig,L}^n (\tilde{T}_L^{s,n+1} - \tilde{T}_{g,L}^{n+1}) - \left(\frac{1-\varepsilon}{2}\right) \Gamma_{w,L}^n (\dot{h}_{g,L}^n - \dot{h}_{f,L}^n) \quad (2.10)$$

The undefined variables are as follows $\tilde{Q}_{ig,L}^{n+1}$ is the volumetric heat addition rate of the interfacing gas in the measured volume at an intermediate time variable; $\dot{h}_{g,L}^n$ is the derivative of the specific enthalpy of the gas in the measured volume at the current time level index; $\dot{h}_{f,L}^n$ is the derivative of the specific enthalpy of the liquid in the measured volume at the current time level index;

The provisional advanced time temperatures

The provisional advanced time temperatures are used to find the new temperature in the next time step. this is done through equation 2.11, equation 2.12, and equation 2.13. this is done by taking the linearization of the temperature states on the previous values. applying it to the linearizing of the phasic properties (equation 2.7, and equation 2.8).

$$\tilde{T}_L^{s,n+1} = T_L^{s,1n} + \left(\frac{\partial T^s}{\partial P}\right)_L^n (P_L^{n+1} - P_L^n) + \left(\frac{\partial T^s}{\partial X_n}\right)_L^n (\tilde{X}_{n,L}^{n+1} - X_{n,L}^n) + \left(\frac{\partial T^s}{\partial U_g}\right)_L^n (\tilde{U}_{g,L}^{n+1} - U_{g,L}^n) \quad (2.11)$$

$$\tilde{T}_{g,L}^{n+1} = T_{g,L}^n + \left(\frac{\partial T_g}{\partial P}\right)_L^n (P_L^{n+1} - P_L^n) + \left(\frac{\partial T_g}{\partial X_n}\right)_L^n (\tilde{X}_{n,L}^{n+1} - X_{n,L}^n) + \left(\frac{\partial T_g}{\partial U_g}\right)_L^n (\tilde{U}_{g,L}^{n+1} - U_{g,L}^n) \quad (2.12)$$

$$\tilde{T}_{f,L}^{n+1} = T_{f,L}^n + \left(\frac{\partial T_f}{\partial P}\right)_L^n (P_L^{n+1} - P_L^n) + \left(\frac{\partial T_f}{\partial U_f}\right)_L^n (\tilde{U}_{f,L}^{n+1} - U_{f,L}^n) \quad (2.13)$$

The undefined variables are as follows $T_L^{s,1n}$ is the temperature of the saturation

property within the measured volume in the initial time step; $(\frac{\partial T^s}{\partial P})_L^n$ is the partial derivative of the temperature of the saturation properties with respect to the pressure within the measured volume at the current time junction; $(\frac{\partial T^s}{\partial X_n})_L^n$ is the partial derivative of the temperature of the saturation properties with respect to the mass fraction of the noncondensable gas within the measured volume at the current time junction; $X_{n,L}^n$ is the mass fraction of the noncondensable gas within the measured volume at the current time junction; $(\frac{\partial T^s}{\partial U_g})_L^n$ is the partial derivative of the temperature of the saturation properties with respect to the specific internal energy of the gas within the measured volume at the current time junction; $T_{g,L}^n$ is the temperature of the gas at the current time junction; $(\frac{\partial T_g}{\partial P})_L^n$ is the partial derivative of the temperature of the gas with respect to the pressure within the measured volume at the current time junction; $(\frac{\partial T_g}{\partial X_n})_L^n$ is the partial derivative of the temperature of the gas properties with respect to the mass fraction of the noncondensable gas within the measured volume at the current time junction; $(\frac{\partial T_g}{\partial U_g})_L^n$ is the partial derivative of the temperature of the gas with respect to the specific internal energy of the gas within the measured volume at the current time junction; $\tilde{T}_{f,L}^{n+1}$ $T_{f,L}^n$ is the temperature of the fluid within the measured volume at an intermittent time step at the current time level index; $(\frac{\partial T_f}{\partial P})_L^n$ is the partial derivative of the temperature of the liquid with respect to the pressure within the measured volume at the current time junction; $(\frac{\partial T_f}{\partial U_f})_L^n$ is the partial derivative of the temperature of the liquid with respect to the specific internal energy of the gas within the measured volume at the current time junction;

2.3.3 Modifications

There are several modifiers that can be added to the model as needed. The main modifiers for the RELAP5-3D program are as follows. Noncondensable gases are

commonly known as contaminated in the system. An example would be carbon dioxide in a steam turbine system. Next modifier boron concentration in the liquid; this is a common neutron-absorbing molecule that is infused with many control rods for reactors. Over time more particles are worn away into the cooling fluid. The small particles can absorb energy in the fuel, and alter the efficiency of the model.

The next modifier is the radionuclide transport model, this is the evaluation of the cooling fluid's changes and effects due to molecules in the fluid being irradiated. Lastly stratified flow, this modification is applicable for any sector in a model where the flow velocity is low relative to its viscosity and density. The common term would be where the fluid settles. This phenomenon alters the boundary layer size and creates a more unique flow pattern.

CHAPTER 3

Natural Convection

Also known as free convection, natural convection can be measured in multiple different equations. The driving force for free convection or natural convection will be the same in any format. The driving force of natural convection is the pressure difference between two different areas of fluid. In this modeling example, the ohmic heater heats up the fluid in the reactor volume. As the fluid heats up the molecules attempt to expand. This in turn causes the pressure to increase in the reactor volume. At the same time, the heat exchanger volume has water running through the copper piping creating a tube and shell heat exchanger. This setup creates a location that will continuously drive the fluid to the ambient temperature within the shell.

Over time the pressure will increase in the reactor volume until it reaches a tipping point. The forces of increased pressure will overcome the static forces of the system. When this happens small fluid convection systems start to form, also known as eddies, within the reactor volume. As the pressure continues to increase the size and number of eddies increase. If the system continues to heat up and build pressure, there starts to be a flow that runs through the complete closed system.

As the reactor volume continues to heat up the flow will increase until the majority of the fluid is running through the system. Natural convection, or free convection, has been achieved.

As the energy input in the system increases the flow through the system will increase, and as the energy input decreases the flow of the fluid will also decrease. If the energy input remains the same the mass flow rate will be the same throughout the system. The major limiting factor is the vaporization of the fluid running through the system.

If the temperature and pressure increase enough to turn the fluid into a gas it greatly complicates the model. A mixed of saturated fluid is outside of the scope of this project so the program is run within the liquid state of water. There were spaces that did flash to steam in small pockets of the model and this is addressed in the pressurizer section. Adding a compressible fluid to the system changes the heating rate of the fluid. This also changes the heat transfer rate due to equation 3.1.

$$h = \frac{q}{\Delta T} \quad (3.1)$$

where h is the heat transfer coefficient q is the heat flux and ΔT is the temperature difference between the surface and the fluid; This can also be broken down in Newton's law of cooling rate equation 3.2

$$Q = h * A(T(t) - T_{fluid}) \quad (3.2)$$

where h is the heat transfer coefficient, A is the heat transfer area, $T(t)$ is the temperature of the surface, and T_{fluid} is the temperature of the fluid

3.1 Modeling Equation

3.1.1 Navier–Stokes and first law of thermodynamics

The Navier-Stokes equation is based on the momentum of the fluid in a model. At the core, the Navier-Stokes equation is 3.3

$$\frac{\delta(\rho u)}{\delta t} + \frac{\delta(\rho u^2)}{\delta x} + \frac{\delta(\rho uv)}{\delta y} + \frac{\delta(\rho uw)}{\delta z} = -\frac{p}{\delta x} + \frac{1}{Re_f} \left(\frac{\delta\tau_{xx}}{\delta x} + \frac{\delta\tau_{xy}}{\delta y} + \frac{\delta\tau_{xz}}{\delta z} \right) \quad (3.3)$$

Where ρ is the density of the fluid; t is the time step within the equation. with x , y , and z being the coordinates within the fluid. u is the velocity component in the x -direction; v is the velocity component in the y -direction; w is the velocity component in the z -direction. With p being the pressure within the system. Re_f being the Reynolds number within the fluid. and τ being the stress factor within the specific coordinates.

This is the base equation for the momentum in the x coordinates with two similar equations for the y and z coordinates. This equation can be complex due to the eight separate partial differential equations involved within a single plane of the modeling. To simplify the Navier-Stokes equation there are three components that can be assumed.

First, the model is isothermal outside of the heat exchanger segment. There is some heat transfer that happens between the outer wall of the model and the ambient air. Due to the scope of this project the complexity of free convection in an open space, and the minimal amount of energy lost in the system compared to the level of accuracy of the testing equipment provided the model can be viewed as isothermal outside of the heat transfer within the heat exchanger. The second component that is assumed is the state of the fluid running through the system. The model is designed to never let the liquid within the system reach the vaporization point. Due to that system design, the model can be assumed to be a liquid throughout the system, and in turn, it can be assumed that the fluid will be compressible.

Third, the last assumption that is made is the density of the fluid in the system. With the primary coolant staying in one state the density of that coolant will generally normalize throughout the system. That allows the assumption that the primary fluid is at a constant viscosity. With those three assumptions, the Navier-Stokes equation

can be simplified down to 3.4

$$\rho \frac{\delta \vec{V}}{\delta t} = -\vec{\nabla} P + \rho \vec{g} + \mu \nabla^2 \vec{V} \quad (3.4)$$

where ρ is the density of the fluid; \vec{V} is the absolute velocity. t is the time step of the system. With $\vec{\nabla} P$ being the Pressure difference over the vector quantity; \vec{g} being the gravitational acceleration. lastly the $\mu \nabla^2 \vec{V}$ is the Laplacian of the velocity components.

3.1.2 Churchill-Chu Natural Convection Evaluation

Also known as the Churchill-Bernstein correlation. The Churchill-Chu Natural Convection equation is focused on the convection of a fluid normally around a hot object. The Churchill-Chu equation is the evaluation of a vertical plate. If the Reynolds number and Prandtl number of the fluid are within a range greater than 0.2 the Churchill-Chu equation is a valid evaluation. The equation can be shown in 3.5

$$\overline{Nu}_L = \left(0.825 + \frac{0.387 Ra_L^{1/6}}{[1 + (\frac{0.492}{Pr})^{9/16}]^{8/27}} \right)^2 \quad (3.5)$$

where \overline{Nu}_L is the Nusselt number; Pr is the Prandtl number of the fluid, and Ra_L is the Rayleigh number of the fluid. Turbulence is not a direct result of buoyancy, but of instabilities (traditional view) or chaotic interactions among vertical structures

McAdam's Natural Convection for horizontal Evaluation

McAdam's natural convection equation is based around a flat horizontal plate, in stark contrast to the Churchill-Chu Equation which is designed around a flat vertical

plate. There are two forms of this equation. The first for this equation is where the upper surface of the hot plate is hot, or the lower surface of the plate is cold. This equation can be displayed as 3.6 and 3.7

$$\overline{Nu}_L = 0.54Ra_L^{1/4} (10^4 \lesssim Ra_L \lesssim 10^7) \quad (3.6)$$

$$\overline{Nu}_L = 0.15Ra_L^{1/3} (10^5 \lesssim Ra_L \lesssim 10^{11}) \quad (3.7)$$

The other form of McAdam's Equation is designed for evaluating the bottom surface of a hot plate, or the top surface of a cold plate. This equation can be displayed as 3.8

$$\overline{Nu}_L = 0.27Ra_L^{1/4} (10^5 \lesssim Ra_L \lesssim 10^{10}) \quad (3.8)$$

Both McAdam's and Churchill-Chu's equation is designed for a model that is two dimensions.

CHAPTER 4

Natural Convection Model

4.1 Overview

The RELAP5-3D model is composed of seven main components separated into separate RELAP5-3D cards. The six main components can be seen in Figure 1.1 with the last component being the pressurizer. Each component has ten nodes that allow the system to separate the evaluation of each component.

The RELAP5-3D model is modeled in one dimension to simplify complications and focus on the scope of the project, natural convection. The elements are condensed down to the water in both liquid and steam states. The only point of heat loss is contained within the heat exchanger section of the model. The only point of heat addition is contained within the reactor section of the model. The remaining volumes in the model only can transfer heat and mass through the connected volumes.

The remainder of the sections can not transfer energy in or out of the system. The only mass transfer out of the scope of the model is the tube side of the heat exchanger. Due to the steady state of the mass flow rate of the tube side of the heat exchanger the model will continue to have the same mass at any time step during the execution of the program.

4.2 Juncture and branches

There are two junctures and two branches within the model. Figure 1.1 shows the components in reference to the surrounding components. Both components have Isothermal walls, with only mass and energy transfer allowed through the connec-

tions to the other components. Both components contain ten nodes within their structuring.

The two branches are labeled the return and chimney. The return is an annulus that is wrapped around the heater component. The chimney is a pipe that is attached to the top of the heater. The two junctures are the top branch and the bottom branch. Both connect the annulus to the inner pipe. The only thing that differs is the top branch. The top branch is connected to the pressurizer above it.

4.2.1 Pressurizer

The Pressurizer is attached to the top of the model. It was added to allow the program to run correctly without crashing. The physical model is an open container. Allowing any steam or gases to escape the model through the top branch. To simplify this behavior in the RELAP5-3D model a pressurizer was added and partially filled with saturated steam. This did two things for the model. This creates a mimicked open-air top to the container.

The second thing that the pressurizer does is allows normalization of the pressure for the model. This allows for any part of the fluid to flash to gas and allows for expansion in the in-compressible fluid. without this addition, the program will crash if any of the contained fluids changes to gas through pressure or temperature change.

Adding the pressurizer and creating a closed pressurized system creates two restrictions. The first restriction only allows water to be contained within the system. This does not allow nitrogen or any atmospheric gas to be added to the model. It also won't allow the model to exhibit electrolyzation where the hydrogen atoms separate from the oxygen atoms. This phenomenon was witnessed when the physical model was created. Due to the scope of this model being focused on the natural convection

of the fluid and not the interaction with other elements pressurizer is a good solution to the problem.

4.2.2 Heat Exchanger Volume

The heat exchanger is a simple shell and tube configuration. The tube configuration is built in the same manner as the physical model. the tube is made of copper with a total length of 1.524 meters. The cross-sectional area of the tube is 0.000247 meters squared. The volume flow rate of the fluid running through the tube is $0.000451 \frac{m^3}{sec}$. That is approximately 0.119048 US Gallons per second. The fluid running through the tube side is standing water.

The heat exchanger is built and designed to have a steady state flow throughout the execution of the program. Outside of the energy loss through the tube of the heat exchanger, there is no other mass or heat transfer that takes place within the heat exchanger section of the model. the heat exchanger is built as a standard counterflow heat exchanger. This is where the entrance of the hot side, or the shell, is located to the exit of the cold side, or tube.

4.2.3 Reactor

The reactor section of the program is a standard branch with a heater element within it. The heater element needs to mimic the conductive nodes that are in the physical model. the RELAP5-3D Model mimics this performance by having a single heater element in the center of the reactor volume. The heater element is a cylinder style with an extremely small radius. This long thin cylinder will create the best heating profile without an obstacle that will restrict the flow of fluid around it.

To help reduce the chances of the fluid flashing to steam the energy was added equally between ten nodes within the heater element. This differs from the way ohmic heaters react in a fluid. The other difference from the physical model is the lack of electrolyzing in the fluid. Due to the scope of this project being focused on the natural circulation of the model this deviation is acceptable.

4.2.4 Time Step

The RELAP5-3D code was not able to be run in a complete format. Figure 4.1 shows the graphical values of the result of an execution of this code. The upper left graph is the mass flow rate of the primary throughout the experiment. The upper right graph shows the temperature in both the hottest space and the coolest. The hottest location is the node just above the reactor volume, with the coolest location being just below the heat exchanger volume. The lower left graph shows energy being put in at each step. Notice there are four distinct time steps. Finally, the bottom right graph shows the pressure in the chimney volume of the program.

As can be seen the upper right mass flow rate is very sporadic and unpredictable. As the energy input and energy removal from the system are constant the mass flow rate should work its way to a steady state flow. As the graph shows during each power increase step, there is no sign of that happening.

The temperature increases and the mass flow rate increases with more energy being added to the system. That behavior matches the physical model. The pressure also remains consistent throughout the execution of the program. There were a series of tests to ensure that the program is running correctly and that what was exhibited is not a flaw in the design of the code.

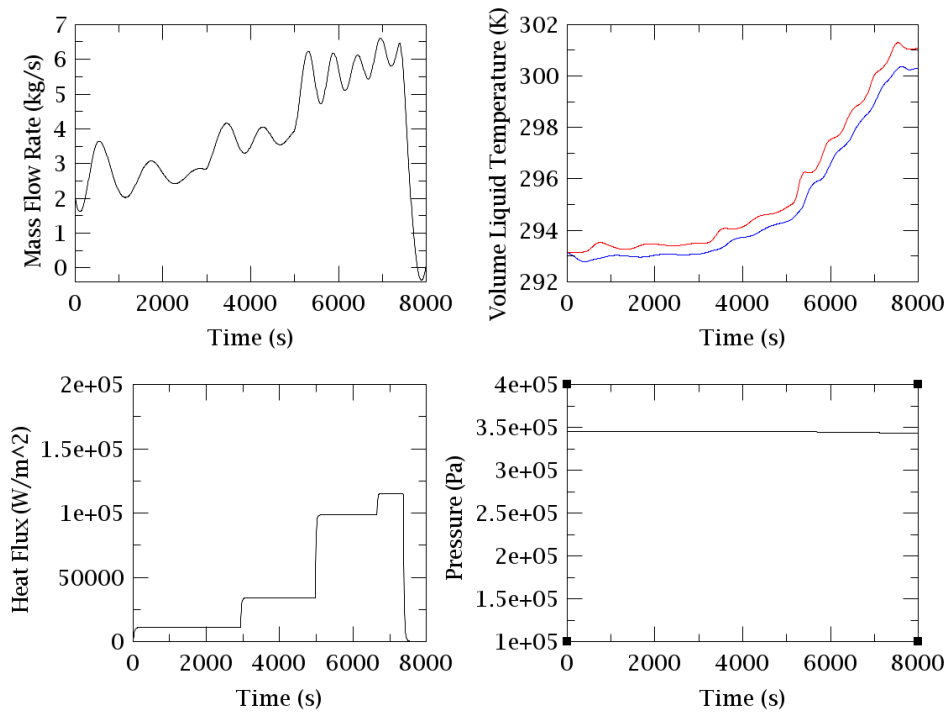


Figure 4.1: Graphical returned values of a continuously running program

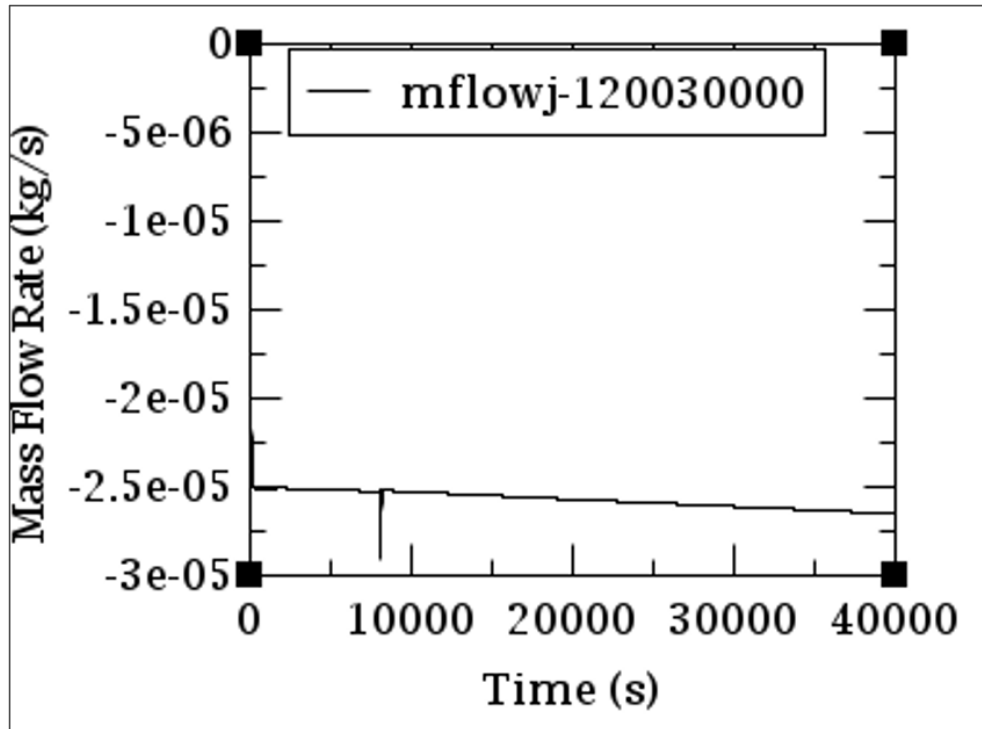


Figure 4.2: Mass flow rate of the model with no reactor

Isothermal Integrity

To ensure there was only one point that adds energy to the system and one point where the heat is removed from the system, there were two tests conducted.

The first test removed the heater element in the reactor volume of the model. Doing this allows a simple observation. If the program has no mass flow and no heat gains or losses the model has only one point of energy being put in the model. It will also show that the pressurizer is not complicating the flow. This can be seen from Figure 4.2 where the mass flow rate of the top branch is fundamentally zero.

The second test was required to disconnect the cold line from the heat exchanger volume. This will ensure that the model will not lose heat or energy in any other volumes. This will ensure that the heat exchanger is the only location to remove heat

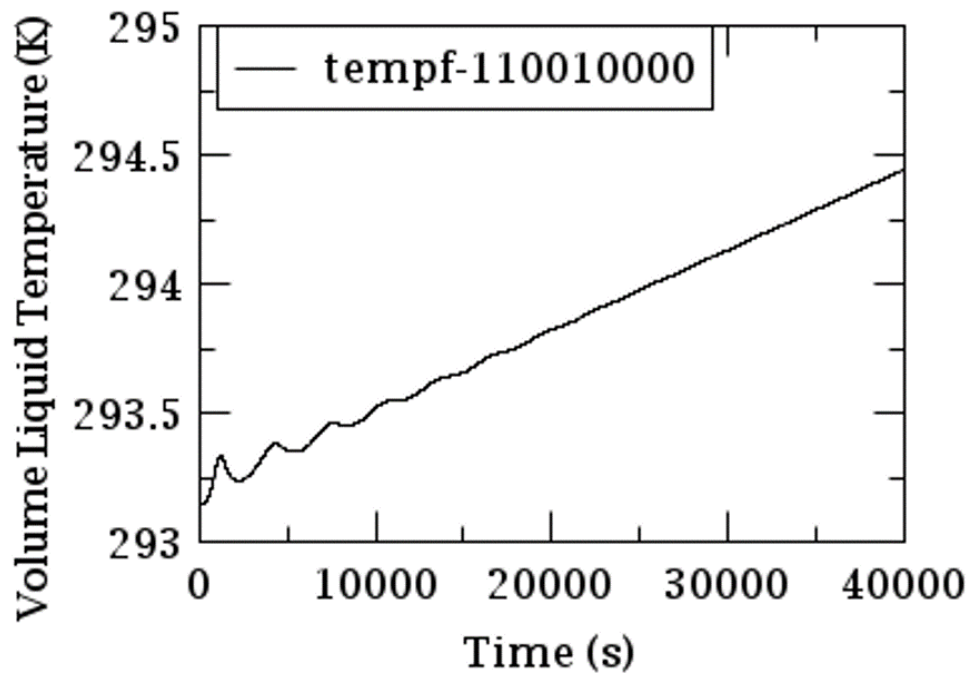


Figure 4.3: Temperature of the model without the heat exchanger

from the model. This test can be graphically viewed with Figure 4.3. The heater unit continues to input energy into the reactor volume. As seen in Figure 4.3 the temperature is increasing at a steady and stable rate. This shows that the model is isothermally contained. That shows the only way to remove heat into the model is through the heat exchanger.

Short Timed Single Step

With the model being proven to be thermally sound the program can be run without the time steps. This will provide preliminary data. This can be seen graphically in Figure 4.4. Figure 4.4 shows the mass flow rate of the chimney volume. As it can be observed it moved from zero to a steady flow rate of $1 \frac{Kg}{Sec}$. There is a variant of the

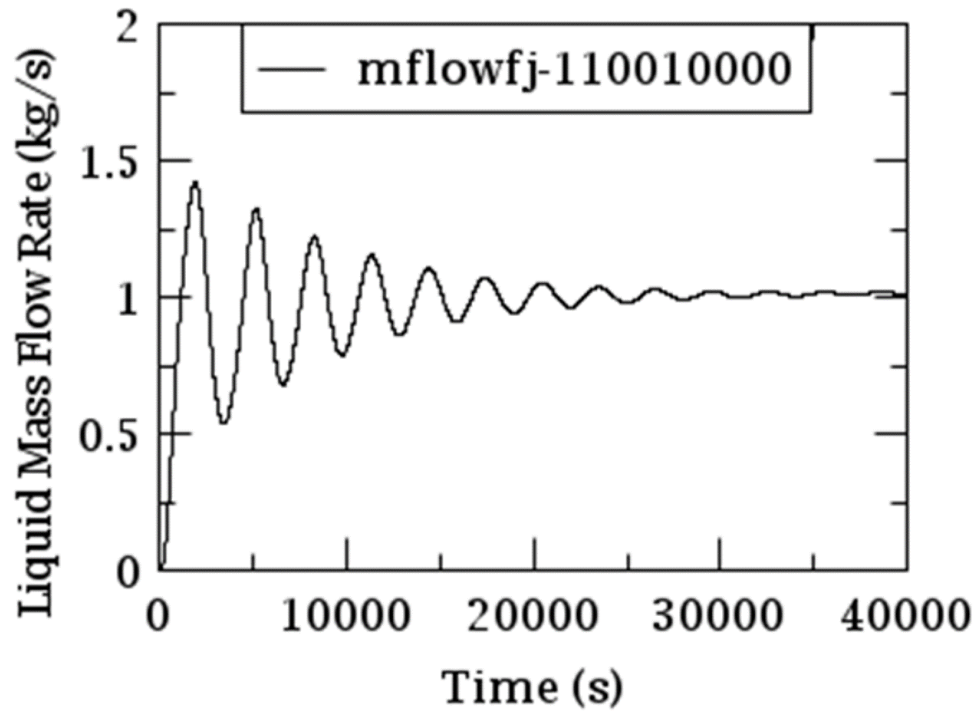


Figure 4.4: Temperature of the model without the heat exchanger

mass flow rate oscillating; this will be addressed later in the paper.

CHAPTER 5

Resulting Data

5.1 Time Stepped Model

The time step model has been broken up into 4 separate codes. The separate codes are divided by wattage put into the system; the first being 500 Watts, then 1,542 Watts, the third 4,452 Watts, and lastly 5,200 Watts. Figure 5.1 shows the overlay of all the mass flow rates of every time step, they're logarithmic trend-line

The first time step can be seen in Figure 5.2 where this measures the mass flow rate of the coolant water in kilograms per second. As seen in the figure the mass flow rate increases to nearly 4 kilograms per second and then oscillates down nearly 1.8 kilograms per second. As time goes on the oscillations minimize and the mass flow rate begins to move to a steady state. This follows the natural convection behavior that is expected.

The only difference is the oscillating behaviors that appear throughout all four of the different power settings. Taking the logarithmic trend line of the data points creates a smoother and more accurate evaluation of what happens in the physical model. this can be seen by the dotted lines in Figure 5.2

Table A.1 shows the numerical values of the power input, mass flow rate (center of the chimney volume), the cold temperature (top of the return volume), the hot temperature (bottom of the chimney), and the temperature difference between the hot and the cold. Similar to the mass flow rate both the hot and cold temperatures oscillate during the beginning of the operation, but as time passes the temperatures normalize to 293.32 K and 293.74 K respectively. The temperature differences start at an unstable and relatively high value at the beginning of the program, but as the

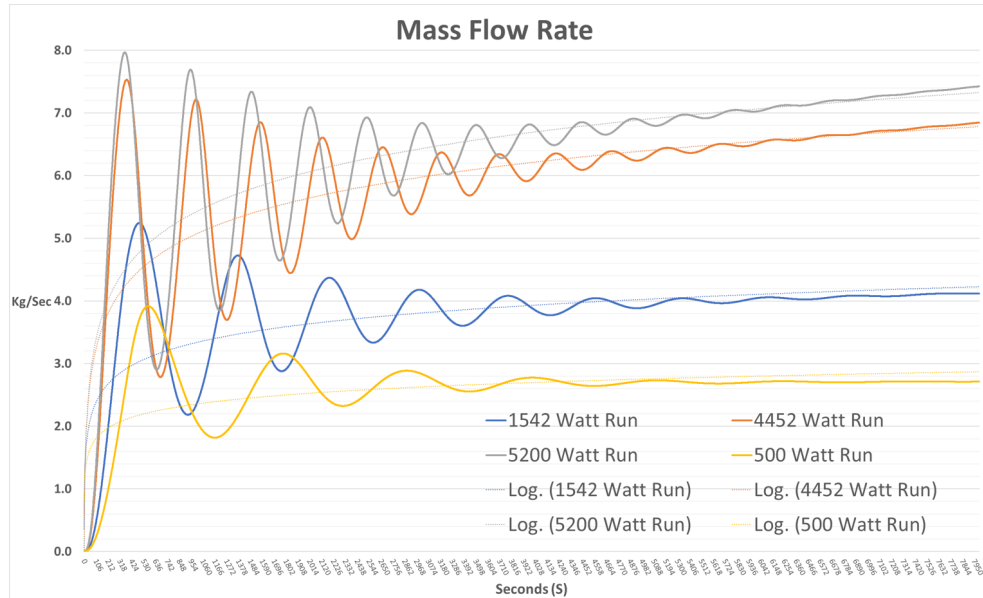


Figure 5.1: Mass Flow Rate at all wattage

temperatures stabilize the temperature differences hold steady at 0.42 K.

The second time step has a constant power input of 1542 Watts. It follows a similar trend line as the first model at 500 Watts with both the oscillations and the normalizing behaviors at the end of the program. Figure 5.3 visually shows the mass flow rate in kilograms per second, where the high peak of the oscillation is near 5.2 kilograms per second, and the mass flow rate leveling to 4.11 kilograms per second. As with the first time step taking the logarithmic trend line will show a closer behavior to the physical model

Table A.2 shows the numeric values for the second time step. Table A.2 has the same values and evaluation locations as Table A.1. as seen in Table A.2 the hot temperature normalizes at 297.61 kelvin with a temperature difference of 0.72 K from the cold side.

The third and final time steps ran consistently at 4452 Watts and 5200 Watts respectively. Figure 5.4 and Table A.3 show the values for the third time step run-

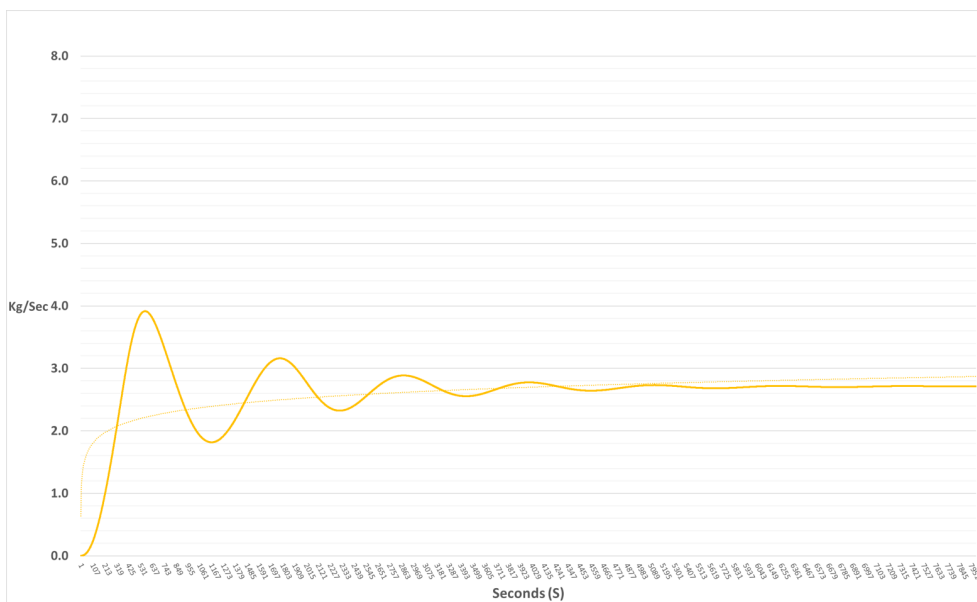


Figure 5.2: Mass Flow Rate at 500 Watts

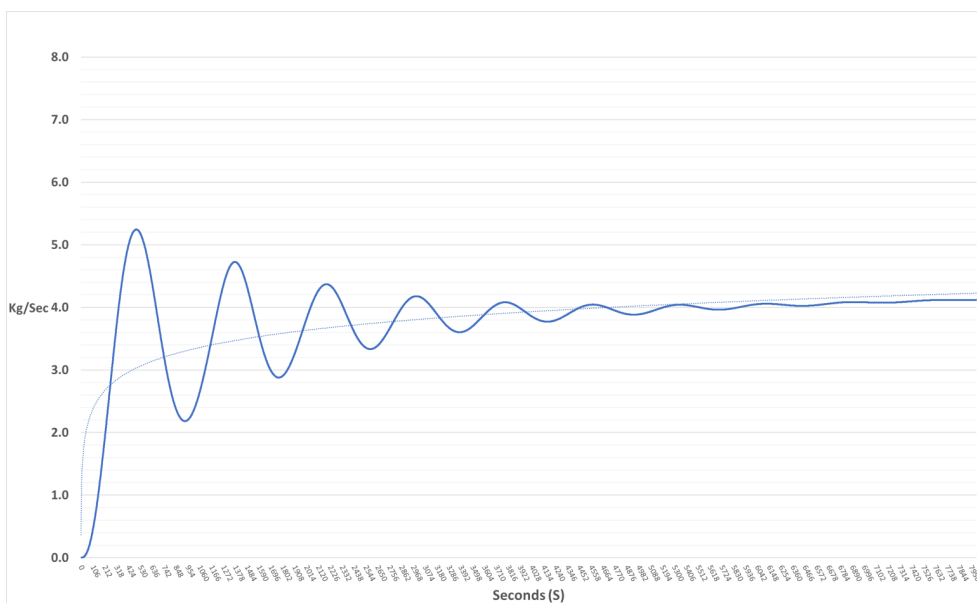


Figure 5.3: Mass Flow Rate at 1542 Watts

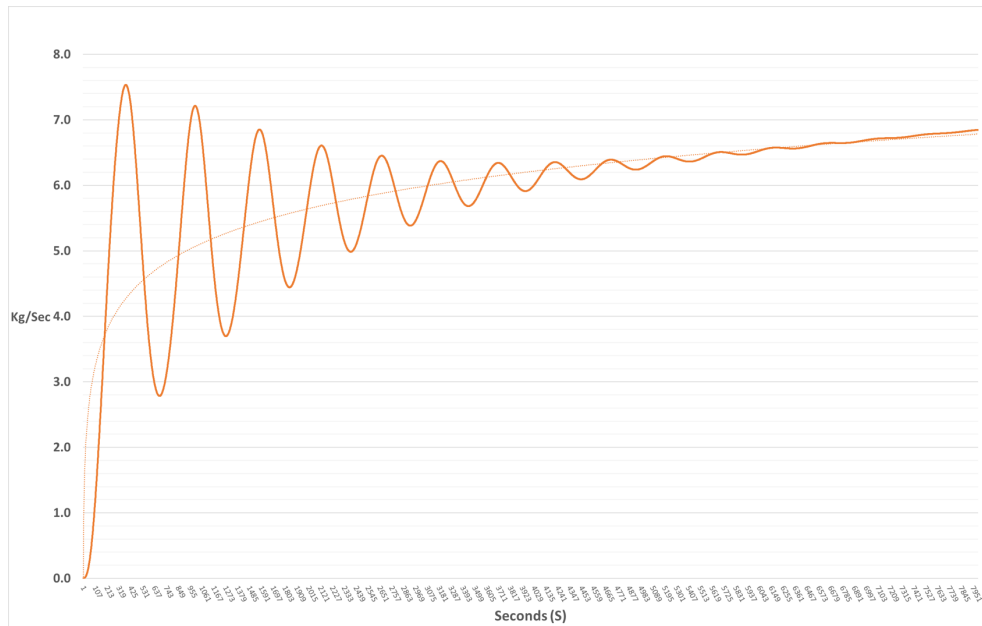


Figure 5.4: Mass Flow Rate at 4452 Watts

ning at 4452 Watts. The oscillation peak for the mass flow rate is approximately 7.5 kilograms per second with a temperature difference of 1.21 K at the end of the program.

With Figure 5.5 and Table A.4 show the values for the final time step running at 5200 Watts. The oscillation peak for the mass flow rate is approximately 8 kilograms per second with a temperature difference of 1.3 K at the end of the program.

There is one main difference between these two programs from the earlier time steps. The heat exchanger is not removing enough energy from the system to let the mass flow rate move to a steady state. This also makes the hot and cold temperatures slowly increase by approximately 0.1 Kelvin per minute.

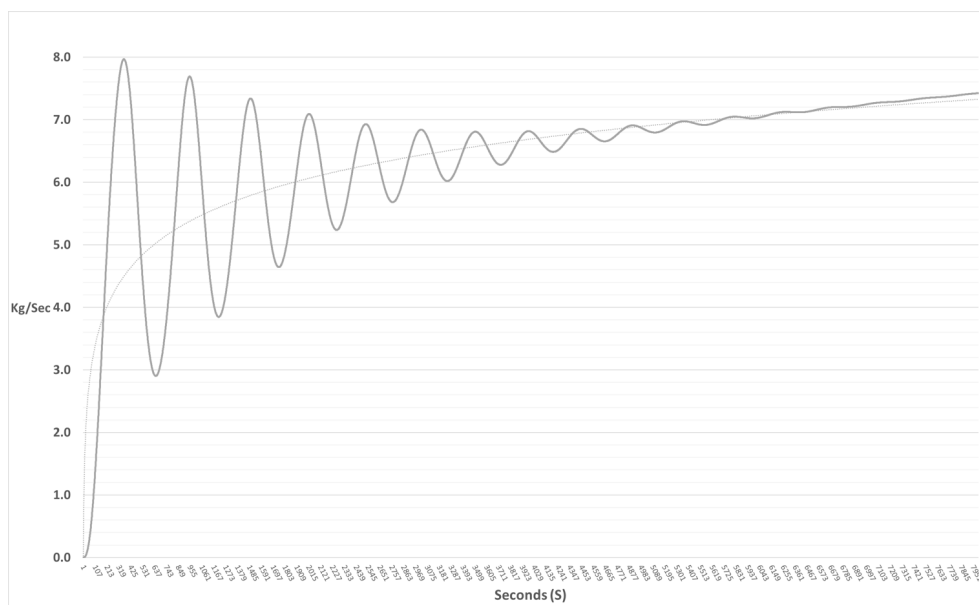


Figure 5.5: Mass Flow Rate at 5200 Watts

CHAPTER 6

Hand Calculation

6.1 Equation

Ideally, the physical model would be the most equivalent comparison to the RELAP 3D model. Unfortunately, the physical model had thermal data gather, but never had the mass flow rate or volume flow rate measured. For a point of reference, hand calculations were performed. The hand calculation can be performed using the Momentum Equation seen in equation 6.1

$$\sum \vec{F} = \sum_{out} \beta \dot{m} \vec{V} - \sum_{in} \beta \dot{m} \vec{V} \quad (6.1)$$

where the \vec{F} is the body forces applied to control volume in the x direction β is the momentum flux, \dot{m} is the mass flow rate and \vec{V} is the velocity of the fluid in the x direction

With some modification, the equation 6.1 can be modified to an integrated loop momentum equation. the integrated loop momentum equation can be displayed as equation 6.2 where

$$\frac{d\dot{m}}{dt} \sum_i \frac{l_i}{a_i} = (\rho_c - \rho_h)gH - \frac{1}{2} \sum_i \left(\frac{fl}{d_h} + K \right)_i \rho_i v_i^2 \quad (6.2)$$

where \dot{m} is the mass flow rate of the system, the $\frac{d\dot{m}}{dt}$ is the derivative of the mass flow rate of the fluid in reference to the time of t. the \sum_i is the sum of all parts that make up the whole system. l_i is the length of the given section of i . a_i is the cross-sectional area of the given section of i . ρ_c is the density of the coldest section of the system, with ρ_h being the density of the hottest section of the system. g is the

gravitation acceleration rate. H is the height difference between the coldest section of the system and the hottest section of the system. f is the friction factor of the section of i . d_h is the hydraulic diameter of the section of i . With K being the minor losses due applied to the particular section of i . leaving the ρ_i and v_i to be the density of and the velocity of the section of i respectively.

These integrated loop momentum equations can be used to evaluate the same model that RELAP 3D created. Evaluating the system when it has reached its steady state balance will help to eliminate the derivative of the mass flow rate. When the integrated loop momentum equation is at steady state $\frac{dm}{dt}$ is set to zero and creates equation 6.3

$$gH(\rho_c - \rho_h) = \frac{1}{2} \sum_i \left(\frac{fl}{d_h} + K \right)_i \rho_i v_i^2 \quad (6.3)$$

To be able to evaluate a one-to-one comparison there are only needs to be things. the first is assumed that in a close-looped system all \dot{m}_i are equal to each other. the second is inserting equation 6.4 in to equation 6.3 to replace all v_i .

$$v_i = \frac{\dot{m}}{\rho_i a_i} \quad (6.4)$$

6.2 Execution and Resulting Data

For the hand calculations, the model was divided in half vertically. That is based on the evaluation that the model has a vertical symmetrical flow. This will allow the removal of any branching that would be required to be modeled, and intern simplifying the problem

The hand calculation was divided into the same 6 volumes as the model. This can

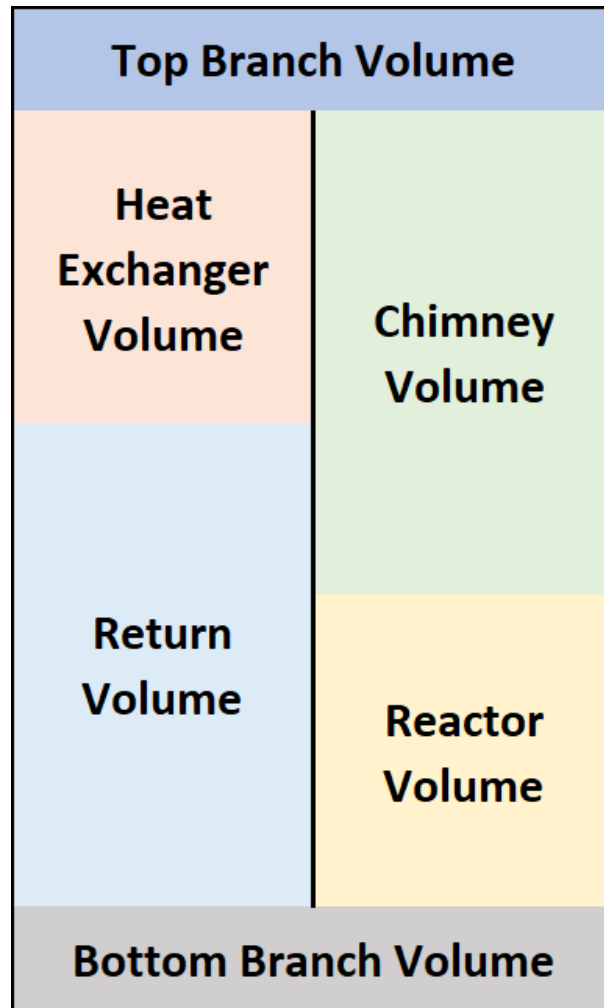


Figure 6.1: Volume configuration of the hand calculations

be seen in Figure 6.1, where the center for the hottest volume is the reactor volume, and the center for the coldest volume is the heat exchanger volume.

The Friction Factor for the calculation was based on the Reynolds number of the fluid in that section. With the heat exchanger built like the RELAP 3D model has it been created? the heat exchanger is a single copper pipe that runs vertically with the model. this creates the simplest comparison due to the dimension. To compensate for that model the cross-sectional area of the heat exchanger volume was reduced,

RELAP 3D Mass flow rate	
4.1205	Kg/Sec
Hand Calculation Mass Flow Rate	
0.56663	Kg/Sec

Figure 6.2: Comparative mass flow rates

and the hydraulic diameter is increased

When the hand calculation equation is processed for the mass flow rate of a steady state system the value is found to be $0.5663 \frac{Kg}{Sec}$ when compared to the RELAP 3D model it has an error rate of 86%. Figure 6.2 compares the mass flow rate found in the RELAP 3D model verse the hand calculations. This is a considerable deviation from the modeling data. There are a few possible explanations as to why.

The first possible explanation is the evaluation of the friction factor. In the RELAP 3D model the friction factor is evaluated through the roughness of the pipe, the shape of the volume, and any possible objects that are contained within that volume. The hand calculation only uses the Reynolds number. Another variation that is found within the two different evaluations is the turn loss coefficient. In the hand calculations, there is no evaluation of the change in the flow structures in each of the volumes for any change in geometry. In RELAP 3D there is a more complicated governing equation that allows for the evaluation of the geometry of each volume.

These other differences are less noticeable but should still be mentioned. The first minor difference is the presence of a pressurizer in the RELAP 3D model. In the hand calculations, there can be volumes that have 100% of the space filled with fluid. The RELAP 3D program required a pressurizer to be able to normalize pressure spikes, and in turn, keep the program from crashing. This shouldn't play a major factor in the evacuation difference due to the time delay to steady state. When the RELAP 3D

program runs until the system is in a steady state the fluid and energy transfer to the pressurizer is driven to zero. The next minor difference is the ambient temperature outside the system. The last minor difference is the number of minor volumes that are divided in the RELAP 3D program. The hand calculation has the same number of volumes as the RELAP 3D program, but in the program, each volume is cut into 10 smaller sub-volumes. The variation in the temperature between the sub-volumes is small enough that it would not greatly affect the total results.

6.3 Physical Model Comparison

When comparing the RELAP data to the physical model the results from the 40-amp test are the most reliable. The physical model had multiple thermal couples on the outside of the model. the only two data thermal couples that demonstrated accurate data while the omic heating was being produced were the Thermal couples 9 and 10.

Those thermal couples were at the very top of the model on either side between the heat exchanger volume, and the top branch volume in figure 1.1. applying the know amperage and voltage the wattage is approximately 600 watts. this is close to the lowest power RELAP model of 500 watts. Figure 6.3 shows the result of the thermal couples. It can show a relative start temperature of approximately 29 degrees Celsius, with an end temperature of approximately 32 degrees Celsius.

When observing the same location in the 500-wattage RELAP model the start temperature is at 20 degrees Celsius, with an end temperature of 20.4 degrees Celsius. this can be seen in figure 6.4. The same oscillations are seen with the temperature profile as the mass flow rate profile. A few notable differences between the two models can be seen. The physical model has a much higher steady-state temperature. This is

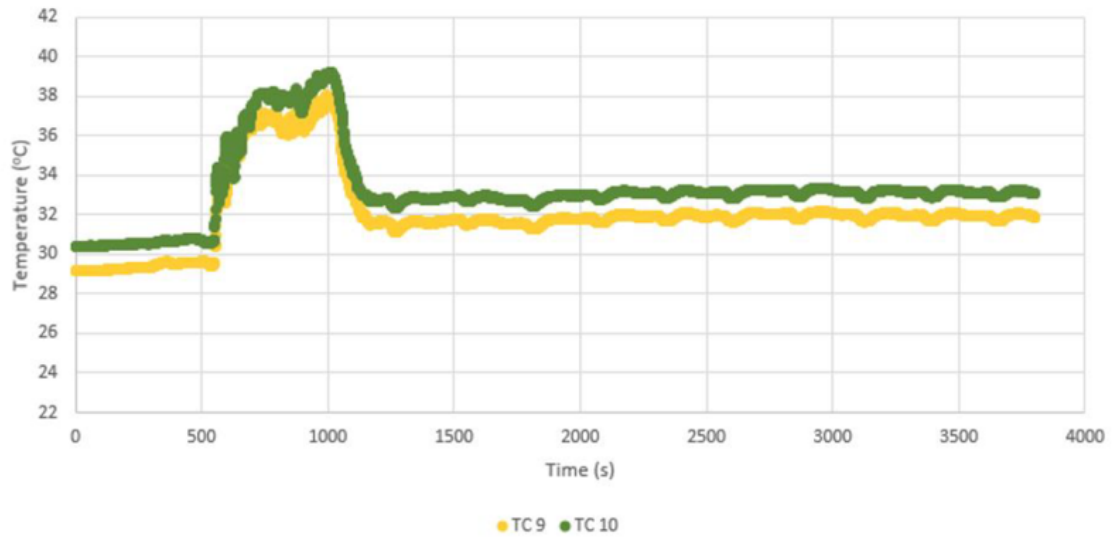


Figure 6.3: Physical model at 40 amps

expected as there is heat loss through the model through the outer walls of the model, the inner walls of the model, and the open-air top. In addition, the majority of the temperature change happens within the first 1500 seconds of the physical model. This can be accounted for due to the static forces being greater for an object at standstill compared to the object in motion. Just like a block being pulled, the amount of force required to get the block to move is greater than the amount of force required to maintain its motion.

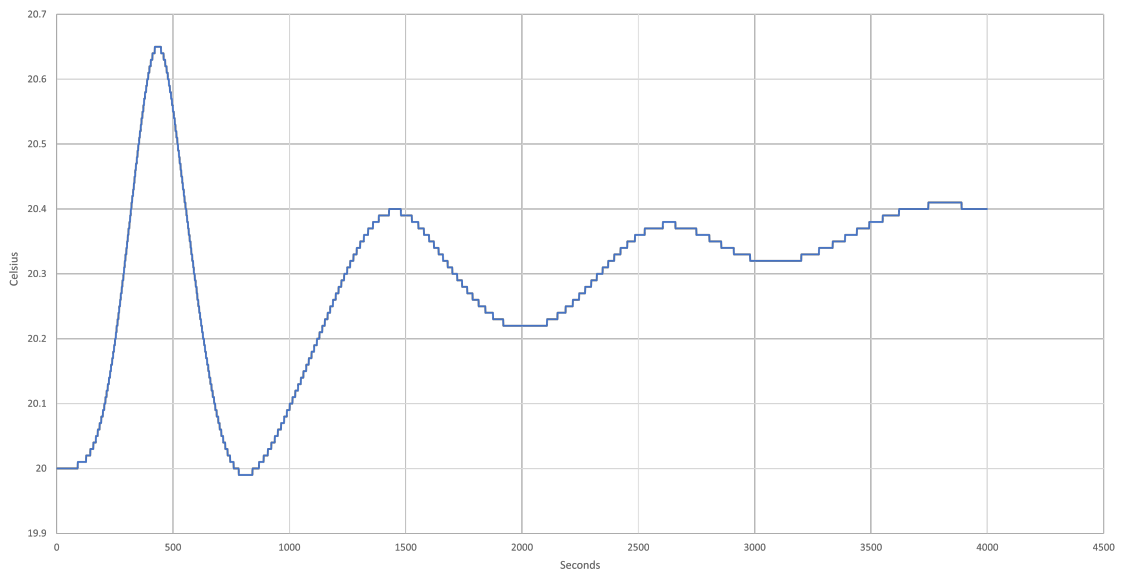


Figure 6.4: RELAP temperature profile of the 500 watt run

CHAPTER 7

Summary and Conclusions

With the data seen in this paper, it is shown that RELAP 3D can effectively be used to model natural convection. There is no need to use a pseudo-pump to compensate for the governing equations that fail to calculate, including pressure differences to create fluid flow. It also displays the correct flow direction of the natural. With the heated fluid rising from the reactor volume, and the cool fluid dropping from the heat exchanger volume.

The data shows a very realistic environment for the physical model. With the hottest part of the model existing in the reactor space, and the coldest fluid existing in the heat exchanger space. The mass flow rate of the RELAP 3D at steady state is $4.12 \frac{Kg}{Sec}$ which is a velocity of $0.05261 \frac{meter}{Sec}$ within the inner pipe. that is a flow rate of about one foot in 5.8 seconds. When the clear plastic model was running the flow rate looked very similar to what the model created.

The RELAP 3D model showed a very strong example of the ramp-up process of the model. The only thing that does not match reality is the oscillations that are visible throughout all of the different wattage inputs. The most likely reason for this is the relatively low energy input into the RELAP 3D program. With the RELAP 3D program most of the energy inputs are much higher input. With salt melting at approximately 800 Celsius the nuclear evaluations are designed to be much higher, with a greater temperature difference between the hottest and coldest parts of the coolant.

Another reason for the oscillations is the evaluation of a one-dimension model. This will only let the fluid move along one axes at a time. Because of this, the RELAP 3D one-dimensional modeling can not account for the small eddies that form

within the volume spaces. This can create a binary response to the evaluation, and in turn, create the oscillations that are seen in the model. There are multiple different future evaluation points that can base on knowing that the RELAP 3D software can use natural circulation as the driving force for a coolant. The first would be validating the model compared to physical models to see if the mass flow rate is accurate. Another would be to use the model to evaluate the natural circulation with a nuclear core and a coolant that can retain more heat. This is the greatest advantage of computer modeling. It allows for more modeling to be created at a fraction of the cost. This in turn creates the opportunity to create a more efficient and practical physical model that will allow more accurate data.

References

- [1] K. M. Bukhari and R. T. Lahey, "The Measurement of Countercurrent Phase Separation and Distribution in a Two-Dimensional Test Section," **Rensselaer Polytechnic Institute**, Department of Nuclear Engineering, NUREG/CR-3577, January, (1984).
- [2] C.B. Davis, "Assessment of RELAPS-3D Using Data from Two-Dimensional RPI Flow Tests, "Proceedings from the 1998 RELAP5 International Users Seminar. College Station, Texas, May 21, (1998)
- [3] R. M. Al-Chalabi, et al., "NESTLE: A Nodal Kinetics Code," Transactions of the American Nuclear Society, Volume 68, June, (1993).
- [4] H. Finnemann and A. Galati, "NEACRP 3-D LWR Core Transient Benchmark - Final Specifications," NEACRP-L-335 (Revision 1) , January , 1992.
- [5] J. L. Judd, W. L. Weaver, T. Downar, and J. G. Joo, "A Three Dimensional Nodal Neutron Kinetics Capability for RELAP5," Proceedings of the 1994 Topical Meeting on Advances in Reactor Physics, Knoxville, TN, April 11-15, (1994), **Vol. II**, pp 269-280.
- [6] G. L. Mesina, "Border-Profile LU Solver for RELAP5-3D," Proceedings of the 1998 RELAP5 International Users Seminar, College Station, Texas, May 17-21, (1998).
- [7] J. A. Findley and G. L. Sozzi, "BWR Refill Reflood Program Model Qualification Task Plan," EPRI NP 1527, NUREG CR 1899, GEAP 24898, October 1981.

- [8] T. M. Anklam, R. J. Miller, M. D. White, "Experimental Investigation of Uncovered Bundle Heat Transfer and Two-Phase Mixture Level Swell Under High-Pressure and Low Heat Flux Conditions," NUREG CR-2456, ORNL-5848, March 1982. RELAP5-3D GWJ 2015 36
- [9] K. Carlson, R. Riemke, R. Wagner, J. Trapp, "Addition of Three-Dimensional Modeling," RELAP5/TRAC-B International Users Seminar, Baton Rouge, LA, November 4-8, 1991.
- [10] R. Riemke, "RELAP5 Multi-Dimensional Constitutive Models," RELAP5/TRAC-B International Users Seminar, Baton Rouge, LA, November 4-8, 1991.
- [11] K. Carlson, R. Riemke, R. Wagner, "Theory and Input Requirements for the MultiDimensional Component in RELAP5 for Savannah River Site Thermal-Hydraulic Analysis," EGG-EAST-9878, Idaho National Engineering Laboratory, July, (1992).
- [12] K. Carlson, C. Chou, C. Davis, R. Martin, R. Riemke, R. Wagner, "Developmental Assessment of the Multi-Dimensional Component in RELAP5 for Savannah River Site Thermal-Hydraulic Analysis," EGG-EAST-9803, Idaho National Engineering Laboratory, July, (1992).
- [13] K. Carlson, C. Chou, C. Davis, R. Martin, R. Riemke, R. Wagner, R. Dimenna, G. Taylor, V. Ransom, J. Trapp, "Assessment of the Multi-Dimensional Component in RELAP5/MOD2.5, Proceedings of the 5th International Topical Meeting on Nuclear Reactor Thermal-Hydraulics", Salt Lake City, Utah, USA, September 21-24, 1992.

- [14] P. Murray, R. Dimenna, C. Davis, "A Numerical Study of the Three Dimensional Hydrodynamic Component in RELAP5/MOD3," RELAP5 International Users Seminar, Boston, MA, USA, July, (1993).
- [15] G. Johnsen, "Status and Details of the 3-D Fluid Modeling of RELAP5," Code Application and Maintenance Program Meeting, Santa Fe, NM, October, (1993).
- [16] E. Tomlinson, T. Rens, R. Coffield, "Evaluation of the RELAP5/MOD3 Multi-dimensional Component Model", RELAP5 International Users Seminar, Baltimore, MD, August 29 -September 1, (1994).
- [17] A. Shieh, "1D to 3D Connection for the Nearly-Implicit Scheme," INEL Report, June, (1997).
- [18] K. Carlson, "1D to 3D Component Connection for the Semi-Implicit Scheme," INEL Report, June, (1997).
- [19] C. Davis, "Assessment of the RELAP5 Multi-Dimensional Component Model Using Data from LOFT Test L2-5," INEEL Report LDRD 3101, September, (1996).
- [20] R. M. Al-Chalabi, et al, "NESTLE: A Nodal Kinetics Code," Transactions of the American Nuclear Society, **Volume 68**, June, (1993).
- [21] H. Finnemann and A. Galati, "NEACRP 3-D LWR Core Transient Benchmark-Final Specifications," NEACRP-L-335 (Revision 1), January, (1992).
- [22] J. L. Judd, W. L. Weaver, T. Downar, J. G. Joo, "A Three Dimensional Nodal Neutron Kinetics Capability for RELAP5," Proceedings of the 1994 Topical

- Meeting on Advances in Reactor Physics, Knoxville, TN, April 11-15, 1994, **Vol. II**, pp 269- 280.
- [23] H. Finnemann, et al, "Results of LWR Core Transient Benchmarks," Proceedings of the Joint International Conference on Mathematical Methods and Supercomputing in Nuclear Applications, **Vol. II**, pg. 243, Kernforschungszentrum, Karlsruhe, Germany, April, (1993)
- [24] V. H. Ransom, Course A-Numerical Modeling of Two-Phase Flows for Presentation at Ecole d'Ete d'Analyse Numerique, EGG-EAST-8546, Idaho National Engineering Laboratory, May (1989).
- [25] M. Ishii, Thermo-Fluid Dynamic Theory of Two-Phase Flow, Collection de la Direction des Etudes et Recherches d'Electricite de France, (1975).
- [26] F. H. Harlow and A. A. Amsden, "Flow of Interpenetrating Material Phases," Journal of Computational Physics, 18, (1975), pp. 440-464.
- [27] P. S. Anderson, P. Astrup, L. Eget, and O. Rathman, "Numerical Experience with the Two-Fluid Model RISQUE," Proceedings from Topical Meeting on Thermal Reactor Safety, Sun Valley, ID, July 31-August 4, (1977).
- [28] N. Zuber, "On the Dispersed Two-Phase Flow in the Laminar Flow Regime," Chemical Engineering Science, 19, (1964), pp. 897-917.
- [29] L. Van Wijngaarden, "Hydrodynamic Interaction between Gas and Bubbles in Liquid," Journal of Fluid Mechanics, 77, 1, (1976), pp. 27-44.

- [30] R. T. Lahey, Jr., "RPI Two-Phase Flow Modeling Program," Fifth Water Reactor Safety Research Information Meeting, Washington, D.C., November 7-11, (1977).
- [31] D. A. Drew, L. Y. Cheng, and R. T. Lahey, Jr., "The Analysis of Virtual Mass Effects in Two-Phase Flow," *International Journal of Multiphase Flow*, 5, (1979), pp. 233-242.
- [32] J. P. Holman, *Heat Transfer*, 4th Edition, New York: McGraw-Hill, 1976, pp. 244-245, 280.
- [33] Das, Debayan, Roy, Monisha, Basak, Tanmay. (2017). Studies on natural convection within enclosures of various (non-square) shapes-A review. *International Journal of Heat and Mass Transfer*, 106, 356-406.
- [34] Hedayat, Afshin. (2017). Simulation and transient analyses of a complete passive heat removal system in a downward cooling pool-type material testing reactor against a complete station blackout and long-term natural convection mode using the RELAP5 3.2 code. *Nuclear Engineering and Technology*, 49(5), 953-967.
- [35] M. Pons, P. Le Quere. "Modeling Natural Convection with the work of pressure-forces a thermodynamic necessity" *International Journal of Numerical Methods for Heat Fluid Flow*, **173** 322-332. (2007)
- [36] Weber, D. D. (1980). Similitude modeling of natural convection heat transfer through an aperture in passive solar heated buildings. University of Idaho.
- [37] Parvin, Salma, Nasrin, Rehena, Alim, M.A, Hossain, N.F, Chamkha, Ali J. (2012). Thermal conductivity variation on natural convection flow of water-

alumina nanofluid in an annulus. *International Journal of Heat and Mass Transfer*, 55(19-20), 5268-5274.

- [38] K.A. Brucker, J. Majdalani Equivalent thermal conductivity for compact heat sink models based on the Churchill and Chu correlation. *IEEE Transactions on Components and Packaging Technologies*, 158-164

Appendix A: Data from the executed programs

Data from the 500 Watt Program

Table A.1: 500 Watt Time Step

Time (sec)	Power (Watt)	Mass Flow Rate (kg/sec)	Temp Cold (K)	Temp Hot (K)	Temp Diff (Δ K)
0	503.88	0	293.15	293.15	0
60	503.88	0.0642461	293.15	293.15	0
120	503.88	0.29078	293.12	293.16	0.04
180	503.88	0.68276	293.03	293.21	0.18
240	503.88	1.2038	292.91	293.32	0.41
300	503.88	1.8184	292.82	293.49	0.67
360	503.88	2.4868	292.75	293.67	0.92
420	503.88	3.1302	292.71	293.79	1.08
480	503.88	3.6198	292.71	293.75	1.04
540	503.88	3.8771	292.76	293.59	0.83
600	503.88	3.898	292.83	293.43	0.6
660	503.88	3.736	292.88	293.29	0.41
720	503.88	3.4657	292.9	293.19	0.29
780	503.88	3.1467	292.92	293.15	0.23
840	503.88	2.8191	292.95	293.14	0.19
900	503.88	2.5113	292.97	293.17	0.2
960	503.88	2.2449	293	293.21	0.21

Table A.1: 500 Watt Time Step

Time (sec)	Power (Watt)	Mass Flow Rate (kg/sec)	Temp Cold (K)	Temp Hot (K)	Temp Diff (Δ K)
1020	503.88	2.0359	293.02	293.26	0.24
1080	503.88	1.8944	293.03	293.31	0.28
1140	503.88	1.8249	293.03	293.36	0.33
1200	503.88	1.8265	293.03	293.42	0.39
1260	503.88	1.8934	293.02	293.46	0.44
1320	503.88	2.0162	293.02	293.5	0.48
1380	503.88	2.1821	293.01	293.53	0.52
1440	503.88	2.3757	292.99	293.55	0.56
1500	503.88	2.5799	292.98	293.54	0.56
1560	503.88	2.7763	292.97	293.52	0.55
1620	503.88	2.9469	292.96	293.5	0.54
1680	503.88	3.075	292.95	293.47	0.52
1740	503.88	3.1475	292.94	293.44	0.5
1800	503.88	3.1575	292.95	293.41	0.46
1860	503.88	3.1062	292.96	293.39	0.43
1920	503.88	3.0037	292.98	293.37	0.39
1980	503.88	2.8672	293.01	293.37	0.36
2040	503.88	2.7176	293.03	293.37	0.34
2100	503.88	2.5752	293.05	293.37	0.32
2160	503.88	2.4565	293.06	293.39	0.33
2220	503.88	2.3728	293.07	293.41	0.34

Table A.1: 500 Watt Time Step

Time (sec)	Power (Watt)	Mass Flow Rate (kg/sec)	Temp Cold (K)	Temp Hot (K)	Temp Diff (Δ K)
2280	503.88	2.3296	293.07	293.43	0.36
2340	503.88	2.3274	293.07	293.45	0.38
2400	503.88	2.3621	293.06	293.48	0.42
2460	503.88	2.4263	293.06	293.5	0.44
2520	503.88	2.5102	293.05	293.51	0.46
2580	503.88	2.603	293.05	293.52	0.47
2640	503.88	2.6939	293.04	293.53	0.49
2700	503.88	2.7735	293.04	293.52	0.48
2760	503.88	2.8346	293.04	293.51	0.47
2820	503.88	2.8728	293.04	293.5	0.46
2880	503.88	2.8865	293.05	293.49	0.44
2940	503.88	2.8768	293.05	293.48	0.43
3000	503.88	2.8469	293.06	293.47	0.41
3060	503.88	2.8021	293.07	293.47	0.4
3120	503.88	2.7484	293.08	293.47	0.39
3180	503.88	2.6925	293.09	293.47	0.38
3240	503.88	2.6407	293.1	293.48	0.38
3300	503.88	2.5984	293.1	293.49	0.39
3360	503.88	2.5694	293.11	293.5	0.39
3421	503.88	2.5556	293.11	293.51	0.4
3481	503.88	2.5576	293.11	293.52	0.41

Table A.1: 500 Watt Time Step

Time (sec)	Power (Watt)	Mass Flow Rate (kg/sec)	Temp Cold (K)	Temp Hot (K)	Temp Diff (ΔK)
3541	503.88	2.5736	293.11	293.53	0.42
3601	503.88	2.6006	293.11	293.54	0.43
3661	503.88	2.6347	293.11	293.55	0.44
3721	503.88	2.6718	293.11	293.55	0.44
3781	503.88	2.7074	293.11	293.56	0.45
3841	503.88	2.7379	293.11	293.56	0.45
3901	503.88	2.7603	293.11	293.55	0.44
3961	503.88	2.773	293.12	293.55	0.43
4021	503.88	2.7755	293.12	293.55	0.43
4081	503.88	2.7686	293.13	293.55	0.42
4141	503.88	2.7539	293.13	293.55	0.42
4201	503.88	2.7339	293.14	293.55	0.41
4261	503.88	2.7114	293.14	293.55	0.41
4321	503.88	2.6891	293.15	293.55	0.4
4381	503.88	2.6694	293.15	293.56	0.41
4441	503.88	2.6544	293.16	293.57	0.41
4501	503.88	2.6453	293.16	293.57	0.41
4561	503.88	2.6426	293.16	293.58	0.42
4621	503.88	2.6459	293.17	293.58	0.41
4681	503.88	2.6544	293.17	293.59	0.42
4741	503.88	2.6667	293.17	293.6	0.43

Table A.1: 500 Watt Time Step

Time (sec)	Power (Watt)	Mass Flow Rate (kg/sec)	Temp Cold (K)	Temp Hot (K)	Temp Diff (Δ K)
4801	503.88	2.6812	293.17	293.6	0.43
4861	503.88	2.6961	293.17	293.6	0.43
4921	503.88	2.7098	293.18	293.61	0.43
4981	503.88	2.7209	293.18	293.61	0.43
5041	503.88	2.7285	293.18	293.61	0.43
5101	503.88	2.7322	293.18	293.61	0.43
5161	503.88	2.7318	293.19	293.61	0.42
5221	503.88	2.7279	293.19	293.61	0.42
5281	503.88	2.7213	293.2	293.61	0.41
5341	503.88	2.713	293.2	293.62	0.42
5401	503.88	2.7041	293.2	293.62	0.42
5461	503.88	2.6956	293.21	293.62	0.41
5521	503.88	2.6886	293.21	293.63	0.42
5581	503.88	2.6837	293.21	293.63	0.42
5641	503.88	2.6812	293.22	293.63	0.41
5701	503.88	2.6813	293.22	293.64	0.42
5761	503.88	2.6837	293.22	293.64	0.42
5821	503.88	2.688	293.23	293.65	0.42
5881	503.88	2.6936	293.23	293.65	0.42
5941	503.88	2.6998	293.23	293.65	0.42
6001	503.88	2.7058	293.23	293.66	0.43

Table A.1: 500 Watt Time Step

Time (sec)	Power (Watt)	Mass Flow Rate (kg/sec)	Temp Cold (K)	Temp Hot (K)	Temp Diff (Δ K)
6061	503.88	2.7111	293.24	293.66	0.42
6121	503.88	2.7151	293.24	293.66	0.42
6181	503.88	2.7177	293.24	293.66	0.42
6241	503.88	2.7186	293.24	293.67	0.43
6301	503.88	2.718	293.25	293.67	0.42
6361	503.88	2.7161	293.25	293.67	0.42
6421	503.88	2.7132	293.25	293.67	0.42
6481	503.88	2.7099	293.26	293.68	0.42
6541	503.88	2.7066	293.26	293.68	0.42
6601	503.88	2.7036	293.26	293.68	0.42
6661	503.88	2.7014	293.27	293.69	0.42
6721	503.88	2.7	293.27	293.69	0.42
6781	503.88	2.6997	293.27	293.69	0.42
6841	503.88	2.7003	293.28	293.7	0.42
6901	503.88	2.7019	293.28	293.7	0.42
6961	503.88	2.704	293.28	293.7	0.42
7021	503.88	2.7066	293.28	293.71	0.43
7081	503.88	2.7092	293.29	293.71	0.42
7141	503.88	2.7117	293.29	293.71	0.42
7201	503.88	2.7137	293.29	293.71	0.42
7261	503.88	2.7153	293.3	293.72	0.42

Table A.1: 500 Watt Time Step

Time (sec)	Power (Watt)	Mass Flow Rate (kg/sec)	Temp Cold (K)	Temp Hot (K)	Temp Diff (Δ K)
7321	503.88	2.7161	293.3	293.72	0.42
7381	503.88	2.7164	293.3	293.72	0.42
7441	503.88	2.7161	293.3	293.73	0.43
7501	503.88	2.7153	293.31	293.73	0.42
7561	503.88	2.7142	293.31	293.73	0.42
7621	503.88	2.7131	293.31	293.73	0.42
7681	503.88	2.712	293.32	293.74	0.42
7741	503.88	2.7111	293.32	293.74	0.42
7801	503.88	2.7105	293.32	293.74	0.42
7861	503.88	2.7104	293.33	293.75	0.42
7921	503.88	2.7106	293.33	293.75	0.42
7981	503.88	2.7112	293.33	293.75	0.42

Data from the 1542 Watt Program

Table A.2: 1542 Watt Time Step

Time (sec)	Power (Watt)	Mass Flow Rate (kg/sec)	Temp Cold (K)	Temp Hot (K)	Temp Diff (Δ K)
0	1542.5	0	293.15	293.15	0
60	1542.5	0.11675	293.15	293.15	0

Table A.2: 1542 Watt Time Step

Time (sec)	Power (Watt)	Mass Flow Rate (kg/sec)	Temp Cold (K)	Temp Hot (K)	Temp Diff (Δ K)
120	1542.5	0.58828	293.1	293.22	0.12
180	1542.5	1.3846	292.98	293.49	0.51
240	1542.5	2.3759	292.88	293.99	1.11
300	1542.5	3.4165	292.82	294.54	1.72
360	1542.5	4.3318	292.79	294.7	1.91
420	1542.5	4.9599	292.83	294.3	1.47
480	1542.5	5.2343	292.91	293.92	1.01
540	1542.5	5.1423	292.97	293.7	0.73
600	1542.5	4.7315	293.05	293.61	0.56
660	1542.5	4.1163	293.18	293.62	0.44
720	1542.5	3.4446	293.35	293.71	0.36
780	1542.5	2.85	293.48	293.82	0.34
840	1542.5	2.4232	293.57	293.97	0.4
900	1542.5	2.208	293.62	294.13	0.51
960	1542.5	2.2115	293.64	294.3	0.66
1020	1542.5	2.4147	293.64	294.48	0.84
1080	1542.5	2.781	293.63	294.62	0.99
1140	1542.5	3.2599	293.6	294.69	1.09
1200	1542.5	3.7856	293.57	294.67	1.1
1260	1542.5	4.2718	293.53	294.59	1.06
1320	1542.5	4.6151	293.52	294.5	0.98

Table A.2: 1542 Watt Time Step

Time (sec)	Power (Watt)	Mass Flow Rate (kg/sec)	Temp Cold (K)	Temp Hot (K)	Temp Diff (Δ K)
1380	1542.5	4.7252	293.55	294.43	0.88
1440	1542.5	4.5739	293.64	294.38	0.74
1500	1542.5	4.2188	293.76	294.36	0.6
1560	1542.5	3.7735	293.89	294.39	0.5
1620	1542.5	3.355	293.99	294.45	0.46
1680	1542.5	3.0478	294.06	294.54	0.48
1740	1542.5	2.8945	294.1	294.66	0.56
1800	1542.5	2.903	294.12	294.79	0.67
1860	1542.5	3.0553	294.12	294.91	0.79
1920	1542.5	3.3149	294.12	295.01	0.89
1980	1542.5	3.632	294.12	295.06	0.94
2040	1542.5	3.9483	294.12	295.06	0.94
2100	1542.5	4.2041	294.13	295.04	0.91
2160	1542.5	4.3491	294.15	295	0.85
2220	1542.5	4.3559	294.19	294.98	0.79
2280	1542.5	4.2309	294.26	294.97	0.71
2340	1542.5	4.014	294.34	294.98	0.64
2400	1542.5	3.7645	294.43	295.02	0.59
2460	1542.5	3.542	294.5	295.08	0.58
2520	1542.5	3.3909	294.55	295.16	0.61
2580	1542.5	3.3346	294.58	295.25	0.67

Table A.2: 1542 Watt Time Step

Time (sec)	Power (Watt)	Mass Flow Rate (kg/sec)	Temp Cold (K)	Temp Hot (K)	Temp Diff (Δ K)
2640	1542.5	3.3751	294.61	295.33	0.72
2700	1542.5	3.497	294.62	295.41	0.79
2760	1542.5	3.6717	294.63	295.46	0.83
2820	1542.5	3.8625	294.65	295.5	0.85
2880	1542.5	4.0308	294.66	295.51	0.85
2940	1542.5	4.1429	294.69	295.51	0.82
3000	1542.5	4.1783	294.73	295.51	0.78
3060	1542.5	4.135	294.78	295.51	0.73
3120	1542.5	4.0298	294.84	295.53	0.69
3180	1542.5	3.8929	294.9	295.56	0.66
3240	1542.5	3.7588	294.96	295.6	0.64
3300	1542.5	3.6572	295	295.66	0.66
3360	1542.5	3.6071	295.04	295.73	0.69
3420	1542.5	3.6146	295.08	295.79	0.71
3480	1542.5	3.6739	295.1	295.85	0.75
3540	1542.5	3.7693	295.12	295.9	0.78
3600	1542.5	3.8791	295.14	295.94	0.8
3660	1542.5	3.9801	295.17	295.96	0.79
3720	1542.5	4.0517	295.2	295.98	0.78
3780	1542.5	4.0812	295.23	295.99	0.76
3840	1542.5	4.0657	295.28	296.01	0.73

Table A.2: 1542 Watt Time Step

Time (sec)	Power (Watt)	Mass Flow Rate (kg/sec)	Temp Cold (K)	Temp Hot (K)	Temp Diff (Δ K)
3900	1542.5	4.0134	295.32	296.03	0.71
3960	1542.5	3.94	295.37	296.07	0.7
4020	1542.5	3.8649	295.42	296.11	0.69
4080	1542.5	3.8056	295.46	296.15	0.69
4140	1542.5	3.7746	295.5	296.2	0.7
4200	1542.5	3.7766	295.53	296.25	0.72
4260	1542.5	3.8089	295.56	296.3	0.74
4320	1542.5	3.8629	295.59	296.35	0.76
4380	1542.5	3.9259	295.62	296.38	0.76
4440	1542.5	3.9841	295.65	296.41	0.76
4500	1542.5	4.0258	295.68	296.44	0.76
4560	1542.5	4.0438	295.71	296.46	0.75
4620	1542.5	4.0368	295.75	296.48	0.73
4680	1542.5	4.0092	295.79	296.51	0.72
4740	1542.5	3.97	295.84	296.54	0.7
4800	1542.5	3.93	295.88	296.58	0.7
4860	1542.5	3.8991	295.92	296.62	0.7
4920	1542.5	3.8841	295.95	296.67	0.72
4980	1542.5	3.8877	295.99	296.71	0.72
5040	1542.5	3.9083	296.02	296.75	0.73
5100	1542.5	3.9404	296.05	296.79	0.74

Table A.2: 1542 Watt Time Step

Time (sec)	Power (Watt)	Mass Flow Rate (kg/sec)	Temp Cold (K)	Temp Hot (K)	Temp Diff (ΔK)
5160	1542.5	3.9767	296.08	296.82	0.74
5220	1542.5	4.0094	296.11	296.85	0.74
5280	1542.5	4.0323	296.14	296.88	0.74
5340	1542.5	4.0415	296.17	296.91	0.74
5400	1542.5	4.0372	296.21	296.94	0.73
5460	1542.5	4.0221	296.25	296.97	0.72
5520	1542.5	4.0016	296.29	297	0.71
5580	1542.5	3.9817	296.32	297.04	0.72
5640	1542.5	3.9676	296.36	297.08	0.72
5700	1542.5	3.9629	296.39	297.11	0.72
5760	1542.5	3.9685	296.43	297.15	0.72
5820	1542.5	3.983	296.46	297.19	0.73
5880	1542.5	4.0029	296.49	297.22	0.73
5940	1542.5	4.0241	296.52	297.26	0.74
6000	1542.5	4.0421	296.55	297.29	0.74
6060	1542.5	4.054	296.58	297.32	0.74
6120	1542.5	4.0583	296.62	297.35	0.73
6180	1542.5	4.0553	296.65	297.38	0.73
6240	1542.5	4.0473	296.69	297.41	0.72
6300	1542.5	4.0374	296.72	297.44	0.72
6360	1542.5	4.0288	296.76	297.48	0.72

Table A.2: 1542 Watt Time Step

Time (sec)	Power (Watt)	Mass Flow Rate (kg/sec)	Temp Cold (K)	Temp Hot (K)	Temp Diff (Δ K)
6420	1542.5	4.0242	296.79	297.51	0.72
6480	1542.5	4.025	296.82	297.55	0.73
6540	1542.5	4.0314	296.85	297.58	0.73
6600	1542.5	4.042	296.88	297.61	0.73
6660	1542.5	4.0547	296.92	297.65	0.73
6720	1542.5	4.0671	296.95	297.68	0.73
6780	1542.5	4.077	296.98	297.71	0.73
6840	1542.5	4.0831	297.01	297.74	0.73
6900	1542.5	4.0851	297.04	297.77	0.73
6960	1542.5	4.0835	297.08	297.8	0.72
7020	1542.5	4.08	297.11	297.83	0.72
7080	1542.5	4.0761	297.14	297.86	0.72
7140	1542.5	4.0738	297.17	297.9	0.73
7200	1542.5	4.0741	297.21	297.93	0.72
7260	1542.5	4.0774	297.24	297.96	0.72
7320	1542.5	4.0835	297.27	298	0.73
7380	1542.5	4.0913	297.3	298.03	0.73
7440	1542.5	4.0995	297.33	298.06	0.73
7500	1542.5	4.1069	297.36	298.09	0.73
7560	1542.5	4.1125	297.39	298.12	0.73
7620	1542.5	4.1159	297.42	298.15	0.73

Table A.2: 1542 Watt Time Step

Time (sec)	Power (Watt)	Mass Flow Rate (kg/sec)	Temp Cold (K)	Temp Hot (K)	Temp Diff (Δ K)
7680	1542.5	4.1172	297.46	298.18	0.72
7740	1542.5	4.117	297.49	298.21	0.72
7800	1542.5	4.1163	297.52	298.24	0.72
7860	1542.5	4.116	297.55	298.27	0.72
7920	1542.5	4.1169	297.58	298.3	0.72
7980	1542.5	4.1194	297.61	298.33	0.72

Data from the 4452 Watt Program

Table A.3: 4452 Watt Time Step

Time (sec)	Power (Watt)	Mass Flow Rate (kg/sec)	Temp Cold (K)	Temp Hot (K)	Temp Diff (Δ K)
0	4452.8	0	293.15	293.15	0
60	4452.8	0.28885	293.14	293.17	0.03
120	4452.8	1.4711	293.05	293.6	0.55
180	4452.8	3.2789	292.95	294.98	2.03
240	4452.8	5.1546	292.89	296.41	3.52
300	4452.8	6.6363	292.9	295.86	2.96
360	4452.8	7.4593	292.98	294.81	1.83
420	4452.8	7.3097	293.12	294.43	1.31

Table A.3: 4452 Watt Time Step

Time (sec)	Power (Watt)	Mass Flow Rate (kg/sec)	Temp Cold (K)	Temp Hot (K)	Temp Diff (ΔK)
480	4452.8	6.1807	293.55	294.43	0.88
540	4452.8	4.6785	294.11	294.65	0.54
600	4452.8	3.4516	294.48	295.02	0.54
660	4452.8	2.8378	294.67	295.5	0.83
720	4452.8	2.9053	294.74	296.05	1.31
780	4452.8	3.5693	294.75	296.61	1.86
840	4452.8	4.6634	294.68	296.89	2.21
900	4452.8	5.9404	294.57	296.71	2.14
960	4452.8	6.9644	294.49	296.39	1.9
1020	4452.8	7.1647	294.63	296.19	1.56
1080	4452.8	6.4012	295.05	296.1	1.05
1140	4452.8	5.1981	295.51	296.2	0.69
1200	4452.8	4.191	295.81	296.49	0.68
1260	4452.8	3.7201	295.97	296.9	0.93
1320	4452.8	3.8489	296.03	297.37	1.34
1380	4452.8	4.4762	296.03	297.77	1.74
1440	4452.8	5.3959	296.01	297.92	1.91
1500	4452.8	6.305	295.99	297.82	1.83
1560	4452.8	6.8225	296.05	297.66	1.61
1620	4452.8	6.6769	296.26	297.58	1.32
1680	4452.8	5.9774	296.61	297.61	1

Table A.3: 4452 Watt Time Step

Time (sec)	Power (Watt)	Mass Flow Rate (kg/sec)	Temp Cold (K)	Temp Hot (K)	Temp Diff (Δ K)
1740	4452.8	5.1456	296.93	297.79	0.86
1800	4452.8	4.577	297.14	298.08	0.94
1860	4452.8	4.458	297.25	298.44	1.19
1920	4452.8	4.7815	297.3	298.77	1.47
1980	4452.8	5.4051	297.32	298.98	1.66
2040	4452.8	6.0887	297.34	299.01	1.67
2100	4452.8	6.5424	297.41	298.96	1.55
2160	4452.8	6.5516	297.58	298.92	1.34
2220	4452.8	6.139	297.84	298.96	1.12
2280	4452.8	5.5619	298.1	299.1	1
2340	4452.8	5.1192	298.3	299.34	1.04
2400	4452.8	4.989	298.43	299.62	1.19
2460	4452.8	5.1934	298.51	299.89	1.38
2520	4452.8	5.6284	298.56	300.07	1.51
2580	4452.8	6.1059	298.62	300.15	1.53
2640	4452.8	6.4125	298.71	300.16	1.45
2700	4452.8	6.4096	298.87	300.17	1.3
2760	4452.8	6.1255	299.08	300.24	1.16
2820	4452.8	5.7381	299.3	300.39	1.09
2880	4452.8	5.4528	299.47	300.59	1.12
2940	4452.8	5.3931	299.59	300.82	1.23

Table A.3: 4452 Watt Time Step

Time (sec)	Power (Watt)	Mass Flow Rate (kg/sec)	Temp Cold (K)	Temp Hot (K)	Temp Diff (ΔK)
3000	4452.8	5.5674	299.68	301.03	1.35
3060	4452.8	5.8853	299.76	301.18	1.42
3120	4452.8	6.1989	299.84	301.27	1.43
3180	4452.8	6.3633	299.96	301.32	1.36
3240	4452.8	6.3112	300.12	301.38	1.26
3300	4452.8	6.0939	300.3	301.48	1.18
3360	4452.8	5.8449	300.48	301.63	1.15
3420	4452.8	5.6965	300.63	301.81	1.18
3480	4452.8	5.7142	300.74	302.01	1.27
3540	4452.8	5.8792	300.84	302.17	1.33
3600	4452.8	6.1074	300.93	302.3	1.37
3660	4452.8	6.289	301.04	302.38	1.34
3720	4452.8	6.3418	301.17	302.46	1.29
3780	4452.8	6.2555	301.32	302.55	1.23
3840	4452.8	6.0946	301.48	302.67	1.19
3900	4452.8	5.9558	301.63	302.82	1.19
3960	4452.8	5.9126	301.76	302.99	1.23
4020	4452.8	5.9826	301.87	303.15	1.28
4080	4452.8	6.1265	301.97	303.29	1.32
4140	4452.8	6.2719	302.08	303.4	1.32
4200	4452.8	6.3502	302.2	303.49	1.29

Table A.3: 4452 Watt Time Step

Time (sec)	Power (Watt)	Mass Flow Rate (kg/sec)	Temp Cold (K)	Temp Hot (K)	Temp Diff (Δ K)
4260	4452.8	6.3325	302.34	303.58	1.24
4320	4452.8	6.2437	302.48	303.7	1.22
4380	4452.8	6.1442	302.63	303.83	1.2
4440	4452.8	6.0933	302.76	303.98	1.22
4500	4452.8	6.1183	302.87	304.13	1.26
4560	4452.8	6.2047	302.98	304.26	1.28
4620	4452.8	6.308	303.09	304.38	1.29
4680	4452.8	6.3785	303.21	304.48	1.27
4740	4452.8	6.3877	303.34	304.58	1.24
4800	4452.8	6.343	303.47	304.7	1.23
4860	4452.8	6.2804	303.61	304.82	1.21
4920	4452.8	6.2415	303.73	304.95	1.22
4980	4452.8	6.2507	303.85	305.09	1.24
5040	4452.8	6.3041	303.96	305.22	1.26
5100	4452.8	6.3748	304.07	305.34	1.27
5160	4452.8	6.4289	304.19	305.45	1.26
5220	4452.8	6.4446	304.31	305.56	1.25
5280	4452.8	6.4234	304.44	305.67	1.23
5340	4452.8	6.3871	304.57	305.79	1.22
5400	4452.8	6.3633	304.69	305.91	1.22
5460	4452.8	6.3699	304.81	306.04	1.23

Table A.3: 4452 Watt Time Step

Time (sec)	Power (Watt)	Mass Flow Rate (kg/sec)	Temp Cold (K)	Temp Hot (K)	Temp Diff (Δ K)
5520	4452.8	6.406	304.92	306.16	1.24
5580	4452.8	6.4546	305.03	306.28	1.25
5640	4452.8	6.4934	305.15	306.39	1.24
5700	4452.8	6.5078	305.26	306.5	1.24
5760	4452.8	6.4984	305.39	306.61	1.22
5820	4452.8	6.4792	305.51	306.73	1.22
5880	4452.8	6.468	305.63	306.85	1.22
5940	4452.8	6.4763	305.74	306.97	1.23
6000	4452.8	6.5032	305.85	307.09	1.24
6060	4452.8	6.5374	305.96	307.2	1.24
6120	4452.8	6.5645	306.08	307.31	1.23
6180	4452.8	6.5758	306.19	307.42	1.23
6240	4452.8	6.5726	306.31	307.53	1.22
6300	4452.8	6.5641	306.43	307.65	1.22
6360	4452.8	6.562	306.54	307.76	1.22
6420	4452.8	6.5725	306.65	307.88	1.23
6480	4452.8	6.594	306.76	307.99	1.23
6540	4452.8	6.6187	306.87	308.1	1.23
6600	4452.8	6.6377	306.99	308.21	1.22
6660	4452.8	6.6464	307.1	308.32	1.22
6720	4452.8	6.6467	307.21	308.43	1.22

Table A.3: 4452 Watt Time Step

Time (sec)	Power (Watt)	Mass Flow Rate (kg/sec)	Temp Cold (K)	Temp Hot (K)	Temp Diff (Δ K)
6780	4452.8	6.6453	307.32	308.54	1.22
6840	4452.8	6.649	307.44	308.65	1.21
6900	4452.8	6.6609	307.55	308.77	1.22
6960	4452.8	6.6787	307.65	308.88	1.23
7020	4452.8	6.697	307.76	308.98	1.22
7080	4452.8	6.7106	307.87	309.09	1.22
7140	4452.8	6.7177	307.98	309.2	1.22
7200	4452.8	6.7206	308.09	309.31	1.22
7260	4452.8	6.7238	308.2	309.41	1.21
7320	4452.8	6.7311	308.31	309.52	1.21
7380	4452.8	6.7434	308.42	309.63	1.21
7440	4452.8	6.7582	308.52	309.74	1.22
7500	4452.8	6.7721	308.63	309.84	1.21
7560	4452.8	6.7824	308.74	309.95	1.21
7620	4452.8	6.7889	308.84	310.05	1.21
7680	4452.8	6.7938	308.95	310.16	1.21
7740	4452.8	6.8	309.05	310.27	1.22
7800	4452.8	6.8091	309.16	310.37	1.21
7860	4452.8	6.8208	309.26	310.48	1.22
7920	4452.8	6.8332	309.37	310.58	1.21
7980	4452.8	6.8442	309.47	310.68	1.21

Data from the 5200 Watt Program

Table A.4: 5200 Watt Time Step

Time (sec)	Power (Watt)	Mass Flow Rate (kg/sec)	Temp Cold (K)	Temp Hot (K)	Temp Diff (ΔK)
0	5200	0	293.15	293.15	0
60	5200	0.33626	293.14	293.18	0.04
120	5200	1.7096	293.05	293.75	0.7
180	5200	3.749	292.95	295.45	2.5
240	5200	5.7703	292.9	296.87	3.97
300	5200	7.2803	292.93	295.79	2.86
360	5200	7.9623	293.02	294.82	1.8
420	5200	7.4188	293.27	294.55	1.28
480	5200	5.8992	293.89	294.67	0.78
540	5200	4.2692	294.48	295.01	0.53
600	5200	3.1904	294.8	295.5	0.7
660	5200	2.9142	294.94	296.11	1.17
720	5200	3.402	294.98	296.8	1.82
780	5200	4.4874	294.94	297.31	2.37
840	5200	5.916	294.81	297.25	2.44
900	5200	7.2242	294.69	296.85	2.16
960	5200	7.6803	294.79	296.58	1.79
1020	5200	6.9306	295.26	296.45	1.19
1080	5200	5.5547	295.82	296.55	0.73

Table A.4: 5200 Watt Time Step

Time (sec)	Power (Watt)	Mass Flow Rate (kg/sec)	Temp Cold (K)	Temp Hot (K)	Temp Diff (ΔK)
1140	5200	4.383	296.18	296.89	0.71
1200	5200	3.8616	296.36	297.39	1.03
1260	5200	4.0656	296.42	297.96	1.54
1320	5200	4.8562	296.43	298.4	1.97
1380	5200	5.957	296.39	298.5	2.11
1440	5200	6.9522	296.38	298.34	1.96
1500	5200	7.3382	296.49	298.16	1.67
1560	5200	6.8785	296.83	298.1	1.27
1620	5200	5.9134	297.25	298.21	0.96
1680	5200	5.0392	297.57	298.5	0.93
1740	5200	4.6506	297.75	298.91	1.16
1800	5200	4.8421	297.84	299.34	1.5
1860	5200	5.491	297.86	299.65	1.79
1920	5200	6.3219	297.88	299.74	1.86
1980	5200	6.9557	297.94	299.68	1.74
2040	5200	7.0559	298.12	299.62	1.5
2100	5200	6.5915	298.43	299.65	1.22
2160	5200	5.8923	298.75	299.82	1.07
2220	5200	5.3676	298.99	300.1	1.11
2280	5200	5.2508	299.13	300.45	1.32
2340	5200	5.5539	299.21	300.76	1.55

Table A.4: 5200 Watt Time Step

Time (sec)	Power (Watt)	Mass Flow Rate (kg/sec)	Temp Cold (K)	Temp Hot (K)	Temp Diff (ΔK)
2400	5200	6.1169	299.27	300.95	1.68
2460	5200	6.6689	299.34	301.01	1.67
2520	5200	6.9273	299.48	301.01	1.53
2580	5200	6.7655	299.7	301.04	1.34
2640	5200	6.3195	299.97	301.16	1.19
2700	5200	5.8796	300.21	301.38	1.17
2760	5200	5.6835	300.38	301.66	1.28
2820	5200	5.8073	300.49	301.93	1.44
2880	5200	6.169	300.58	302.13	1.55
2940	5200	6.5786	300.67	302.24	1.57
3000	5200	6.8222	300.8	302.3	1.5
3060	5200	6.7793	300.99	302.36	1.37
3120	5200	6.5065	301.21	302.47	1.26
3180	5200	6.1933	301.43	302.66	1.23
3240	5200	6.0253	301.6	302.89	1.29
3300	5200	6.0834	301.73	303.12	1.39
3360	5200	6.3231	301.84	303.31	1.47
3420	5200	6.6102	301.94	303.44	1.5
3480	5200	6.7901	302.08	303.53	1.45
3540	5200	6.7752	302.25	303.62	1.37
3600	5200	6.6	302.45	303.74	1.29

Table A.4: 5200 Watt Time Step

Time (sec)	Power (Watt)	Mass Flow Rate (kg/sec)	Temp Cold (K)	Temp Hot (K)	Temp Diff (Δ K)
3660	5200	6.3921	302.64	303.91	1.27
3720	5200	6.2823	302.8	304.11	1.31
3780	5200	6.3293	302.94	304.32	1.38
3840	5200	6.4995	303.06	304.49	1.43
3900	5200	6.6948	303.18	304.62	1.44
3960	5200	6.8087	303.32	304.73	1.41
4020	5200	6.7892	303.49	304.84	1.35
4080	5200	6.6692	303.67	304.97	1.3
4140	5200	6.5394	303.84	305.13	1.29
4200	5200	6.4855	303.99	305.32	1.33
4260	5200	6.5387	304.12	305.5	1.38
4320	5200	6.6656	304.25	305.65	1.4
4380	5200	6.7929	304.38	305.78	1.4
4440	5200	6.8528	304.53	305.9	1.37
4500	5200	6.8237	304.69	306.02	1.33
4560	5200	6.741	304.85	306.16	1.31
4620	5200	6.6691	305.01	306.32	1.31
4680	5200	6.6585	305.15	306.49	1.34
4740	5200	6.7172	305.29	306.65	1.36
4800	5200	6.8106	305.42	306.79	1.37
4860	5200	6.8867	305.56	306.92	1.36

Table A.4: 5200 Watt Time Step

Time (sec)	Power (Watt)	Mass Flow Rate (kg/sec)	Temp Cold (K)	Temp Hot (K)	Temp Diff (Δ K)
4920	5200	6.9083	305.7	307.05	1.35
4980	5200	6.876	305.86	307.18	1.32
5040	5200	6.824	306.01	307.32	1.31
5100	5200	6.7951	306.16	307.48	1.32
5160	5200	6.8127	306.29	307.63	1.34
5220	5200	6.869	306.43	307.78	1.35
5280	5200	6.9327	306.56	307.92	1.36
5340	5200	6.971	306.7	308.04	1.34
5400	5200	6.9706	306.84	308.17	1.33
5460	5200	6.944	306.99	308.31	1.32
5520	5200	6.9193	307.14	308.45	1.31
5580	5200	6.92	307.28	308.6	1.32
5640	5200	6.9509	307.41	308.75	1.34
5700	5200	6.9967	307.54	308.88	1.34
5760	5200	7.0344	307.68	309.01	1.33
5820	5200	7.0484	307.82	309.14	1.32
5880	5200	7.0403	307.96	309.27	1.31
5940	5200	7.0259	308.1	309.41	1.31
6000	5200	7.0234	308.23	309.55	1.32
6060	5200	7.0408	308.37	309.69	1.32
6120	5200	7.0724	308.5	309.83	1.33

Table A.4: 5200 Watt Time Step

Time (sec)	Power (Watt)	Mass Flow Rate (kg/sec)	Temp Cold (K)	Temp Hot (K)	Temp Diff (Δ K)
6180	5200	7.1036	308.63	309.96	1.33
6240	5200	7.1218	308.77	310.09	1.32
6300	5200	7.1242	308.9	310.22	1.32
6360	5200	7.119	309.04	310.35	1.31
6420	5200	7.1185	309.17	310.49	1.32
6480	5200	7.1301	309.31	310.62	1.31
6540	5200	7.1525	309.44	310.76	1.32
6600	5200	7.1771	309.57	310.89	1.32
6660	5200	7.1948	309.7	311.01	1.31
6720	5200	7.2022	309.83	311.14	1.31
6780	5200	7.2033	309.96	311.27	1.31
6840	5200	7.2058	310.09	311.4	1.31
6900	5200	7.2156	310.22	311.53	1.31
6960	5200	7.2327	310.35	311.66	1.31
7020	5200	7.2522	310.48	311.79	1.31
7080	5200	7.2681	310.61	311.92	1.31
7140	5200	7.2773	310.74	312.04	1.3
7200	5200	7.2821	310.86	312.17	1.31
7260	5200	7.2872	310.99	312.3	1.31
7320	5200	7.2967	311.12	312.43	1.31
7380	5200	7.3108	311.25	312.55	1.3

Table A.4: 5200 Watt Time Step

Time (sec)	Power (Watt)	Mass Flow Rate (kg/sec)	Temp Cold (K)	Temp Hot (K)	Temp Diff (Δ K)
7440	5200	7.3268	311.37	312.68	1.31
7500	5200	7.3407	311.5	312.8	1.3
7560	5200	7.3505	311.62	312.93	1.31
7620	5200	7.3573	311.75	313.05	1.3
7680	5200	7.3642	311.87	313.18	1.31
7740	5200	7.3738	312	313.3	1.3
7800	5200	7.3862	312.12	313.42	1.3
7860	5200	7.3998	312.24	313.55	1.31
7920	5200	7.4121	312.37	313.67	1.3
7980	5200	7.4218	312.49	313.79	1.3